Mark J. Ajluni, P.E.
Nuclear Licensing Director

Southern Nuclear Operating Company, Inc.
40 Inverness Center Parkway
Post Office Box 1295
Birmingham, Alabama 35201

Tel 205.992.7673
Fax 205.992.7885

July 7, 2011

SOUTHERN COMPANY

Docket Nos.: 50-366

NL-11-1081

U. S. Nuclear Regulatory Commission
ATTN: Document Control Desk
Washington, D. C. 20555-0001

Edwin I. Hatch Nuclear Plant – Unit 2
Reactor Pressure Vessel 2N2G Recirculation Inlet Nozzle-To-Safe End Weld
Full Structural Weld Overlay
Crack Growth Calculations and Stress Analysis - Spring 2011 Outage (2R21)

Ladies and Gentlemen:

A small axial flaw was detected in dissimilar metal weld 2B31-1RC-12AR-G-5 during the Hatch Nuclear Plant (HNP) Unit 2 – 2R20 Spring 2009 refueling outage. This weld is an Alloy 182 weld that joins a stainless steel safe-end to the low alloy steel 2N2G Recirculation Inlet nozzle. In the 2R21 Spring 2011 refueling outage, Southern Nuclear Operating Company (SNC) applied a full structural weld overlay (FSWOL) over this weld in accordance with SNC's alternative ISI-ALT-08-02, Version 1. This alternative ISI-ALT-08-02, Version 1, was approved per NRC safety evaluation report (SER) dated June 24, 2009 (Accession Number: ML090340017). SNC alternative ISI-ALT-08-02, Version 1, states (in part):

> "Crack growth calculations will be performed as part of a design package. Flaw characterization and evaluation requirements shall be based on the as-found flaw in the case of a contingency overlay...Crack growth, including both stress corrosion and fatigue crack growth, shall be evaluated in the materials in accordance with IWB-3640. If the flaw is at or near the boundary of two different materials, evaluation of flaw growth in both materials is required. This report will be submitted within 90 days after plant startup."

In addition, SNC alternative ISI-ALT-08-02, Version 1, also states:

> "A stress analysis will be performed that demonstrates that the pressure-retaining components will perform their intended design function with the FSWOL installed. The stress analysis report will include results showing that the requirements of Subarticles NB-3200 and NB-3600 of the ASME Code, Section III are satisfied. The stress analysis will also include results showing that the requirements of IWB-3000 of the ASME Code, Section XI, are satisfied. The results will show that the postulated crack including its growth would not adversely affect the integrity of the overlaid welds. This report will be submitted within 90 days after plant startup."

SNC HNP Unit 2 plant startup occurred on May 3, 2011. The crack growth calculations and stress analysis are provided in Enclosure 1 as committed in SNC alternative ISI-ALT-08-02, Version 1. Enclosure 1 contains the residual stress analysis, evaluation of weld overlay shrinkage stresses, ASME Code stress evaluation, and crack growth evaluation. Enclosure 1 satisfies the crack growth calculations and stress analysis 90-day reporting requirements detailed in the SNC alternative ISI-ALT-08-02, Version 1.

This letter contains no NRC commitments. If you have any questions, please contact Jack Stringfellow at (205) 992-7037.

Respectfully submitted,

Mark J Ajluni

M. J. Ajluni
Nuclear Licensing Director

MJA/CLT/lac

Enclosures: 1. Crack Growth Calculations and Stress Analysis

cc: Southern Nuclear Operating Company
Mr. J. T. Gasser, Executive Vice President
Mr. D. R. Madison, Vice President – Hatch
Ms. P. M. Marino, Vice President – Engineering
RTYPE: CHA02.004

U. S. Nuclear Regulatory Commission
Mr. V. M. McCree, Regional Administrator
Mr. P. G. Boyle, NRR Project Manager
Mr. E. D. Morris, Senior Resident Inspector – Hatch

Edwin I. Hatch Nuclear Plant – Unit 2
Reactor Pressure Vessel 2N2G Recirculation Inlet Nozzle-To-Safe End Weld
Full Structural Weld Overlay
Crack Growth Calculations and Stress Analysis
Spring 2011 Outage (2R21)

Enclosure 1

Crack Growth Calculations and Stress Analysis

Report No.: 0900556.401
Revision No.: 0
Project No.: 0900556
File No.: 0900556-401
March 2010
☒ Q ☐ Non-Q

Weld Overlay Design Report
For the Hatch Nuclear Plant Unit 2
Recirculation Inlet Nozzle N2G Weld 2B31-1RC-12AR-G-5

Prepared for:

Southern Nuclear Operating Company
PO 6081146 (GSA JPC-0028)

Prepared by:

Structural Integrity Associates, Inc.
San Jose, California

Prepared by: _____ Date: 03/03/2010
Charles Fourcade

Prepared by: _____ Date: 03/03/2010
Shu S. Tang, P.E.

Reviewed by: _____ Date: 03/03/2010
Marcos L. Herrera, P.E.

Approved by: _____ Date: 03/03/2010
G. Angah Miessi

Structural Integrity Associates, Inc.

REVISION CONTROL SHEET

Document Number: 0900556.401

Title: Weld Overlay Design Report For the Hatch Nuclear Plant Unit 2 Recirculation Inlet N2G Weld 2B31-1RC-12AR-G-5

Client: Southern Nuclear Operating Company

SI Project Number: 0900556

Section	Pages	Revision	Date	Comments
-	i – vi	0	03/03/10	Initial Issue
1.0	1-1 – 1-2			
2.0	2-1 – 2-2			
3.0	3-1 – 3-28			
4.0	4-1			
5.0	5-1 – 5-14			
6.0	6-1 – 6-23			
7.0	7-1			
8.0	8-1 – 8-2			

Professional Engineer Certification Statement

"Weld Overlay Design Report for the Hatch Nuclear Plant Unit 2 Recirculation Inlet N2G Nozzle N2G Weld 2B31-1RC-12AR-G-5."

I, Marcos Legaspi Herrera, being a duly licensed professional engineer under the laws of the State of California, certify that this document was reviewed by me, and that this document meets the requirements of ASME Section XI (as modified by Southern Nuclear Operating Company alternative ISI-ALT-08-02, Version 1.0) and Section III (Editions and Addenda as referenced in the individual calculations), all as applicable to the specific scope of this report. This report is supplementary to the governing Code Design Reports for the systems and components described herein, and does not invalidate those reports. I further certify that this document is correct and complete to the best of my knowledge and belief, and that I am competent to review this document.

Marcos Legaspi Herrera, P.E.
State of California
Registration Number: M21337
April 16, 2009

Table of Contents

Section Page

1.0 INTRODUCTION 1-1

2.0 ASSESSMENT OF WELD OVERLAY REPAIR 2-1

2.1 Weld Overlay Repair and Design Details 2-1

3.0 RESIDUAL STRESS ANALYSIS 3-1

3.1 Background 3-1
3.2 Technical Approach 3-2
3.2.1 Welding 3-2
3.3 Consideration of Weld Repairs and Welding Parameters 3-3
3.4 Finite Element Model 3-3
3.5 Material Properties 3-4
3.6 Weld Repair and Overlay Stress Analysis Method 3-5
3.6.1 Weld Repair Phase 3-5
3.6.2 Weld Overlay Phase 3-6
3.7 Residual Stress Results 3-7

4.0 EVALUATION OF WELD OVERLAY SHRINKAGE STRESSES 4-1

5.0 ASME CODE STRESS EVALUATION 5-1

5.1 Background 5-1
5.2 Technical Approach 5-1
5.3 Analysis 5-2
5.4 Load Combinations 5-3
5.5 ASME Code Section III Evaluation 5-3
5.5.1 Fatigue Evaluation 5-4
5.6 Results of Analysis 5-5
5.6.1 ASME Code, Section III Evaluation 5-5
5.6.2 Fatigue Evaluation 5-5
5.6.3 Electric Power Uprate (EPU) Considerations 5-5
5.7 Concluding Remarks – Stress Evaluation 5-6

6.0 CRACK GROWTH EVALUATION 6-1

6.1 Background 6-1
6.2 Technical Approach 6-1
6.3 Fatigue Crack Growth 6-1
6.4 IGSCC Flaw Growth 6-3
6.5 Electric Power Uprate (EPU) Considerations 6-5

7.0 SUMMARY AND CONCLUSIONS 7-1

8.0 REFERENCES 8-1

List of Tables

Table Page

Table 3-1: Component Materials 3-8
Table 3-2: Material Properties for SA-533, Grade B, Class 1 (Mn-1/2Mo/1/2Ni)..... 3-9
Table 3-3: Material Properties for SA-240, Type 304 Stainless (18Cr-8Ni)..... 3-10
Table 3-4: Material Properties for SA-508 Grade 2 Class 1 (formerly SA-508 Class 2)..... (3/4Ni-1/2Mo-1/3Cr-V) 3-11
Table 3-5: Material Properties for Alloy 82/182/600 (N06600)..... 3-12
Table 3-6: Material Properties for Alloy 52/52M/52MS/690 (N06690) 3-13
Table 3-7: Yield Strength and Ultimate Strength 3-14
Table 3-8: Assumed Heat Input for ID Repair Welding..... 3-15
Table 3-9: Assumed Heat Input for Weld Overlay Welding 3-15
Table 5-1: Attached Piping Loads 5-7
Table 5-2: Summary of Stress Intensity Limits 5-7
Table 5-3: Code Stress Evaluation for Service Level A/B Loads 5-8
Table 5-4: Code Stress Evaluation for Service Level C/D Loads 5-9
Table 5-5: Event Cycles..... 5-10
Table 5-6: Materials for Fatigue Evaluation..... 5-10
Table 5-7: Fatigue Usage Results 5-11
Table 5-8: Fatigue Usage Using Fatigue Reduction Factor..... 5-12
Table 6-1: Curve-fit Coefficients, Unit Pressure 6-6
Table 6-2: Curve-fit Coefficients, Unit Moment 6-6
Table 6-3: Curve-fit Coefficients, Startup Transient 6-7
Table 6-4: Curve-fit Coefficients, Shutdown Transient 6-7
Table 6-5: Curve-fit Coefficients, Scram Transient 6-8
Table 6-6: Curve-fit Coefficients, Loss of A.C. Power (LOP) Transient..... 6-8
Table 6-7: Curve-fit Coefficients, Normal Operating Conditions 6-9
Table 6-8: Ni-Cr-Fe Fracture Toughness..... 6-9
Table 6-9: Crack Growth Summary..... 6-10

List of Figures

Figure Page

Figure 3-1: Weld Overlay Design 3-17
Figure 3-2: As-Modeled Component Definitions 3-18
Figure 3-3: Finite Element Model of Recirculation Inlet Nozzle 3-19
Figure 3-4: As-Modeled Nuggets for ID Weld Repair and Weld Overlay 3-20
Figure 3-5: Applied Boundary Conditions to the Finite Element Model 3-21
Figure 3-6: ID Weld Repair Residual Stresses 3-22
Figure 3-7: Weld Overlay Residual Stresses at 70°F 3-23
Figure 3-8: Weld Overlay Stresses at 546°F and 1000 psia 3-24
Figure 3-9: ID Surface Axial Stresses 3-25
Figure 3-10: ID Surface Hoop Stresses 3-26
Figure 3-11: Stress Path Definitions 3-27
Figure 3-12: Through-Wall Residual Stress Path Profiles 3-28
Figure 5-1: Sections Used for Section III Evaluation 5-13
Figure 5-2: Material Fatigue Curves 5-14
Figure 6-1: PC-Crack Flaw Models Used in Evaluation 6-11
Figure 6-2: Through-wall Stress Distribution, Unit Pressure 6-12
Figure 6-3: Through-wall Stress Distribution, Unit Moment 6-13
Figure 6-4: Through-wall Stress Distribution, Steady-State 6-14
Figure 6-5: Through-wall Stress Distribution, Startup Transient 6-15
Figure 6-6: Through-wall Stress Distribution, Shutdown Transient 6-16
Figure 6-7: Through-wall Stress Distribution, Scram Transient 6-17
Figure 6-8: Through-wall Stress Distribution, Loss of A.C. Power Transient 6-18
Figure 6-9: Through-wall Stress Distribution, Residual 6-19
Figure 6-10: Stress Intensity Factors (Circumferential Flaw) 6-20
Figure 6-11: Fatigue Crack Growth Results (Circumferential Flaw) 6-21
Figure 6-12: Stress Intensity Factors (Axial Flaw) 6-22
Figure 6-13: Fatigue Crack Growth Results (Axial Flaw) 6-23

1.0 INTRODUCTION

A weld overlay (WOL) repair is designed for the reactor pressure vessel (RPV) Recirculation Inlet Nozzle N2G nozzle-to-safe end dissimilar metal weld (DMW) at Hatch Nuclear Plant, Unit 2 (HNP-2). The original nozzle-to-safe end DMW is fabricated from susceptible Alloy 182 weld metal, and is welded to the low alloy steel reactor vessel nozzle using a joint configuration which includes the original Alloy 182 Ni-Cr-Fe butter on the low alloy steel nozzle preparation. An inside surface-connected axial flaw in the weld and buttering material was reported in February 2009 [9] at this location which is susceptible to intergranular stress corrosion cracking (IGSCC), a known issue for boiling water reactor (BWR) bimetallic Alloy 82/182 welds and sensitized stainless steels.

The design analysis of the weld overlay repair for the Hatch Unit 2 Recirculation Inlet N2G nozzle-to-safe end weld is provided in this report. The analysis is based on plant-specific nozzle geometry and nozzle loadings, using guidance from American Society of Mechanical Engineers (ASME) Section XI Code Case N-740 [6].

Weld 2B31-1RC-12AR-G-5 on nozzle N2G connects a stainless steel safe end to the low-alloy steel recirculation inlet nozzle. The intent of the weld overlay repair design is to address the Alloy 182 material in the weld that is susceptible to intergranular stress corrosion cracking (IGSCC) in the BWR environment. The weld overlay design for weld N2G was developed and documented in Reference 1. The overlay material for the weld overlay will be Alloy 52M, which provides increased resistance to IGSCC.

Weld overlays were first applied in 1982 as a repair for IGSCC in stainless steel piping. The purpose of the repairs of this type was to assure that the pressure boundary satisfied the ASME requirements. In the past, weld overlays were generally applied using the GTAW process with Type 308L welding filler material. Since approximately 1998, many weld overlays have been applied using Alloy 52 family of materials, improved nickel based alloys with high SCC resistance. Application of the weld overlays typically is performed with water backing on the inside of the weld to be repaired, which produces a through-wall temperature gradient. The temperature difference between the inside and the outside surfaces, coupled with the normally

occurring shrinkage of the overlay weld metal, has been shown to produce a highly favorable residual stress distribution in the pipe wall.

Since the application of the first overlays, significant field, analytical, and experimental evidence has been assembled, which verifies that weld overlays are long term repairs. The bases for this include the inherent IGSCC resistance of the weld metal typically used for weld overlay application (Alloy 52 family of materials and Type 308L), the inside surface compressive residual stresses produced in the flawed component by the weld overlay process, advances in the inspectability of weld overlay repaired components and experimental demonstrations of the strength of weld overlays. The weld overlay repair technique for IGSCC flawed pipe welds is based upon the application of weld metal to the outside pipe surface and to either side of the flawed location, extending along the full circumference of the pipe/section. The weld overlay repair performs the following:

1. Provides structural reinforcement of the flawed location, such that adequate load carrying capability is provided, either in the overlay by itself, or in some combination of the overlay and the original pipe wall thickness.
2. Provides a barrier of IGSCC-resistant material to prevent IGSCC propagation into the overlaid weld metal.
3. Produces a compressive residual stress distribution in at least the inner portion of the pipe wall, which will inhibit IGSCC initiation and propagation in the original pipe joint.
4. Prevents local leakage from short axial flaws.

In the weld overlay repair to weld N2G, the weld overlay provides a full replacement pressure boundary, not requiring the original pipe wall to carry any of the loads. It should be noted that HNP-2 has been injecting hydrogen (HWC) since the late 1980's and is expected to continue hydrogen injection in the future along with noble metal injection (NMC). These additional activities provide another potential mitigation measure (besides the beneficial weld overlay residual stress) to mitigate the weld against IGSCC.

2.0 ASSESSMENT OF WELD OVERLAY REPAIR

The WOL repair will be performed in accordance with the ASME Code. The WOL repair design meets the requirements of Section XI of the ASME Code, 2001 Edition through 2003 Addenda [2], as modified by Southern Nuclear Operating Company (SNC) alternative ISI-ALT-08-02, Version 1.0 [3]. The 2001 Edition through 2003 Addenda of Section XI of the ASME Code does not provide for a means of a repair without removal of the flaw or temper bead welding without removal of the weld bead.

Code Case N-504-2 and N-638-1 received regulatory approval as noted in Regulatory Guide 1.147, Revision 15. Code Case N-504-2 provides alternative rules for overlay of Class 1, 2, and 3 austenitic stainless steel piping and N-638-1 provides for a temper bead welding of a cavity. Therefore, the use of these two cases for application of a weld overlay repair over an Alloy 82/182 weld is not permissible without NRC approval. In lieu of obtaining approval to use N-504-2 and N-638-1 for the repair of weld N2G, SNC elected to use ISI-ALT-08-02 [3] which was developed from the technical requirements specified in Code Case N-740 [6]. This alternative is comprehensive and provides the details for the design of the overlay, the acceptance examinations and tests, the fatigue analysis requirements, and flaw growth requirements. Comparison of the technical requirements of ISI-ALT-08-02 versus those in N-504-2 and N-638-1 are provided in the appendices to ISI-ALT-08-02.

In this section, compliance with the requirements of Section XI of the ASME Code is documented, as are the requirements of ISI-ALT-08-02. The designed full structural WOL repair is demonstrated to be fully compliant with USNRC Generic Letter 88-01 [4], NUREG-0313, Revision 2 [5] and with Section XI of the Code as modified by ISI-ALT-08-02 [3].

2.1 Weld Overlay Repair and Design Details

The WOL design satisfies the requirements of IWA-4000 in the Edition and Addenda of Section XI applicable to the plant in-service inspection program or later Edition and Addenda as modified by ISI-ALT-08-02. The Repair Plan also specifies the requirements of IWA-4150 of Section XI, as modified by ISI-ALT-08-02.

1. Weld Materials

The weld overlay design calls for the use of Alloy ERNiCrFe-7A nickel base weld metal (Alloy 52M), consistent with the Alternative [3] for machine Gas Tungsten Arc Welding (GTAW) of the 360° WOL layers.

2. WOL Design Requirements

The weld overlay repair meets the requirements of the 2001 Edition through 2003 Addenda of Section XI [2] of the ASME Code, as modified by ISI-ALT-08-02 [3]. The WOL design is provided in Reference 1.

The WOL design meets the allowable requirements of Section IWB-3640 of Section XI of the ASME Code as specified in ISI-ALT-08-02. The WOL thickness was designed assuming a 100% through-original-pipe-wall (360° fully circumferential) indication for the applicable service level conditions. Figure 3-1 of this report shows the weld overlay design. Reference 1 also presents a calculation for the WOL length on each side of the Alloy 182 dissimilar metal weld (DMW).

3. Inspections for WOL Applications

Per the requirements of ISI-ALT-08-02 [3], the following inspections are required:

(a) Examination of existing weld surface and accept as clean prior to WOL application

(b) A surface exam (PT) of the final repaired area if repair is performed

(c) UT of completed WOL repair

3.0 RESIDUAL STRESS ANALYSIS

3.1 Background

In addition to providing structural reinforcement to the postulated flawed location to meet ASME Code safety margins, the weld overlay produces beneficial residual stress that supports the mitigation of IGSCC. The weld overlay approach has been used in the BWR industry on several hundred occasions. There have been no reports of crack extension after application of the weld overlay. Thus, the compressive stress caused by the weld overlay has been effective in mitigating crack growth in BWRs, confirming its use as a long term repair.

The weld residual stress was determined for the weld overlay design. To obtain a bounding assessment of the impact of the weld overlay on the flawed location, the residual stress assessment must consider residual stresses that existed prior to application of the overlay. Thus, the weld overlay analysis should consider residual stresses that are present due to the as-welded condition and any machining, weld repairs or stress improvement that may have previously occurred.

The original fabrication of welds in some instances involves weld repairs. This is especially true for bimetallic welds with P3 materials, in which case steps are taken to avoid post weld heat treatment after welding. It is assumed that there is a strong possibility that weld repairs could have been performed on this weld during its evolution, even though plant records could not definitely determine the extent of any repair. Due to the significant uncertainty in the initial conditions, the goal was to determine the general effect of the weld overlay on a severe as-welded stress distribution (significant tensile stress on the inside surface) that promotes IGSCC.

For this analysis, the following sequence was used in the analysis:

1) Simulate ID weld repair at DMW location
2) Simulate WOL repair
3) Simulate normal operating conditions (546°F and 1,000 psig [10])

3.2 Technical Approach

3.2.1 Welding

The residual stress due to welding is controlled by the welding parameters, thermal transients due to application of the welding process, temperature-dependent material properties, and elastic-plastic stress reversals. The analytical technique uses finite element analysis to simulate the multipass weld repair and weld overlay processes. In order to reduce computational time, lumped weld bead passes were used in this evaluation. The finite element residual stress analysis is presented in Reference 7.

A two-dimensional, axisymmetric finite element model was developed in Reference 12, using the ANSYS software package [8]. The finite element model consists of a local portion of the vessel shell, cladding, nozzle, thermal sleeve, safe end, attached pipe and pipe weld, DMW and weld butter, an assumed ID repair weld, and the weld overlay.

A thermal analysis is performed to simulate the welding process of the ID weld repair and the welding process of the overlay. A non-linear, elastic-plastic stress analysis is then performed to calculate the resultant residual stress state at various points.

The analysis consists of a thermal pass to determine the temperature response of the model to each individual lumped weld pass as it is added in sequence, followed by an elastic-plastic stress pass to calculate the residual stress due to the temperature cycling from the application of each lumped weld pass. Since the residual stress is a function of the welding history, the stress pass for each lumped pass was applied to the residual stress field induced from all previously applied weld passes.

For the thermal analyses, a relatively low convection heat transfer coefficient of 5.0 Btu/hr-ft^2-°F was conservatively assumed at the surface of the model to simulate a water condition inside the pipe. Lower heat transfer rates in welds produce higher temperatures on the inner portion of the pipe which results in lower residual stress. The value of 5.0 Btu/hr-ft^2-°F is

conservative as it results in under-predicting the beneficial residual stresses from the weld overlay.

After the weld overlay was completed, the model was allowed to cool to a uniform temperature of 70°F, then heated up to the operating temperature (546°F) and pressure (1,000 psig) in order to obtain the residual stresses at cold conditions and the steady-state stresses at normal operating conditions (NOC).

3.3 Consideration of Weld Repairs and Welding Parameters

Because details of any weld repairs are not available, a bounding weld repair assumption was made for this evaluation. The approach used to assess the effectiveness of the weld overlay and determination of the weld residual stress was to perform the analytical evaluation of the weld overlay using the residual stress from a 360° fully circumferential ID weld repair as the initial condition. ID weld repairs are known to develop severe inside surface tensile residual stress fields and can also provide for flaw initiation sites due to grinding and weld defects. Thus, a fully circumferential 50% of wall thickness ID repair was simulated and the resulting stress field is used as the initial stress state for the weld overlay residual stress analysis. The weld repair is included in this analysis to show that the tensile stresses generated by it are mitigated by the WOL. It covers part of the weld butter and original weld, as shown in Figure 3-3 and Figure 3-4. Five weld layers are assumed for the ID weld repair. Four weld layers are assumed for the weld overlay.

The maximum interpass temperature was assumed to be 350°F for both the ID weld repair and the weld overlay. The overlay welding was modeled as progressing from the pipe/safe end side towards the nozzle side of the DMW. A thermal efficiency of 70% was assumed for both the weld repair and overlay welding processes.

3.4 Finite Element Model

A 2-dimensional (2-D) axisymmetric finite element model was developed in Reference 12 for the recirculation inlet nozzle using the ANSYS finite element software package [8]. The finite element

model is constructed using the 4-node structural solid element, PLANE182 (the thermal equivalent for the thermal analyses is PLANE55). Figure 3-2 identifies the different components of the nozzle and repair assembly. The ID weld repair and weld overlay nugget layout used for the residual stress evaluation is shown in Figure 3-4. The model includes:

- A portion of the reactor pressure vessel shell
- Vessel/nozzle cladding
- Vessel shell-to-nozzle weld
- Recirculation inlet nozzle
- Nozzle-to-safe end DMW
- Nozzle weld butter
- The safe end
- A portion of the attached piping
- A portion of the thermal sleeve
- The weld overlay
- A postulated ID weld repair of the nozzle-to-safe end DMW

An ID weld repair is assumed to be applied to the nozzle-to-safe end DMW weld in this analysis to show that the tensile stresses generated by an inside surface weld repair are mitigated by the application of the weld overlay. The depth of the repair is assumed to be half of the original weld thickness with a full circumference (360°) extent to simulate the worst case. It should be noted that the ID weld repair produces a more severe residual stress distribution on the inside surface of the weld.

The finite element model is shown in Figure 3-3. The dimensions of the weld overlay repair are shown in Figure 3-1.

3.5 Material Properties

The material identifications of the various components of the model are obtained per Reference 10, and are specified in Table 3-1.

The temperature-dependent material property values used for the finite element analyses are obtained from Reference 11, and summarized in Tables 3-2 through 3-7. The properties are given for temperatures up to 2500°F. The high temperature properties are necessary for simulating the molten metal for the residual stress analysis. For the ASME Code Section III stress evaluation, only temperatures up to operating temperature are necessary.

The residual stress analysis applies the multi-linear isotropic hardening material behavior available within the ANSYS finite element program [8]. To get the temperature-dependent stress-strain curve for each material, the engineering yield strength (YS) and ultimate tensile strengths (UTS) along with the engineering strain at the ultimate tensile strength are required. Those parameters are obtained from Reference 15 as documented in Reference 11 and listed in Table 3-7.

3.6 Weld Repair and Overlay Stress Analysis Method

3.6.1 Weld Repair Phase

3.6.1.1 Heat Input Simulation

Analytically, the deposition of the weld metal is simulated by imposing a heat generation function on the elements representing the active weld nugget for each weld. In ANSYS, the heat generation (*HGEN*) applied to the weld nuggets is a volumetric energy rate, as energy per volume per time.

The assumed heat input parameters for the ID weld repair are presented in Table 3-8. The assumed heat input parameters for the weld overlay are summarized in Table 3-9. After the completion of each weld, the model is cooled down to a uniform ambient temperature of 70°F.

3.6.1.2 Welding Simulation

The welding simulation is performed through the thermal transient analysis. The simulation of the ID weld repair is applied first. After the ID weld repair is completed, the model is cooled down to a uniform ambient temperature of 70°F. The simulation of the WOL is then performed. After the WOL is completed, the model is cooled to a uniform ambient temperature of 70°F.

3.6.2 Weld Overlay Phase

The same methodology described in Section 3.6.1 is utilized for the WOL process. Figure 3-4 shows the weld nugget simulation. At the end of the WOL, the nozzle is allowed to cool to 70°F.

After the thermal transient analysis, the temperature history is imported into the stress pass to calculate the residual stresses due to the nonlinear, elastic-plastic load/unload stress reversal cycles from the heating and cooling of the weld elements. The model is cooled to a uniform ambient temperature of 70°F after the weld overlay is completed, and then heated to a uniform operating temperature of 546°F along with an operating pressure of 1,000 psi applied to the interior surfaces of the model in order to obtain the combined weld residual, pressure, and thermal stresses at operating conditions.

For the operating condition, an induced end-cap load is applied to the free end of the attached piping in the form of tensile axial pressure the value of which is calculated as follows:

$$P_{\text{end-cap}} = \frac{P \times r_{\text{inside}}^{2}}{\left(r_{\text{outside}}^{2} - r_{\text{inside}}^{2}\right)} = \frac{1000 \times 5.687^{2}}{\left(6.375^{2} - 5.687^{2}\right)} = 3{,}897 \text{ psi}$$

where,

$P_{\text{end-cap}}$ = End cap pressure on piping end (psi)
P = Internal pressure (psi)
r_{inside} = Inside radius of attached piping (in)
r_{outside} = Outside radius of attached piping (in)

In the stress pass analysis, symmetric boundary conditions are applied on the free end of the vessel shell, and the free end of the attached piping is coupled in the axial direction to simulate plane strain conditions. Figure 3-5 shows the applied boundary conditions for the stress pass phase of the analysis. Residual stresses are obtained at 70°F after the WOL is complete.

3.7 Residual Stress Results

Overall stress contours, ID surface stress variations, and through-wall stress profiles for the selected paths are evaluated and discussed here. Figures 3-6 through 3-10 display the axial and hoop residual stress distribution results. Figure 3-6 depicts the axial and hoop residual stress distribution at 70°F following the ID weld repair condition. The axial direction and the hoop direction are with respect to the global coordinate system, where axial stress is SY and hoop stress is SZ. It is shown that extensive tensile axial and hoop residual stresses occur along and near the inside surface in the vicinity of the ID weld repair.

The residual stress distributions due to the application of the weld overlay are presented in Figure 3-7 at room temperature and the stress at normal operating conditions is shown in Figure 3-8. In general, the WOL produces extensive compressive residual stresses on the ID surface of the weld region. After the application of theWOL, both the axial and hoop stresses at 70°F and operating conditions are substantially reduced in the inner portion of the DMW, with the hoop stresses becoming compressive on the inside surface near the DMW.

For a further evaluation of the impact of the WOL, Figures 3-9 and 3-10 present plots of the ID surface stresses as a function of distance from the ID weld repair centerline, for the axial and hoop directions, respectively. The results are plotted for three critical load steps: post-ID weld repair, post-WOL at 70°F, and post-WOL at 546°F/1000 psia. The results indicate that the hoop stresses at steady-state operating conditions (i.e., residual, temperature and pressure) become compressive at the dissimilar metal weld inside surface. The post-WOL axial stresses are also mostly compressive at the ID surface of the weld with a maximum tensile stress of 16 ksi, well below the yield strength of the weld metal. The results suggest that the weld overlay has indeed provided some mitigation to the dissimilar metal weld against IGSCC. Thus, the application of the overlay does in fact create beneficial stresses in the nozzle-to-safe end DMW to help mitigate crack initiation or growth.

In addition, through-wall axial and hoop stress results are extracted near the DMW for various paths defined in Figure 3-11. Hoop and axial stresses from the post-WOL condition at

546°F/1000 psia are obtained along the stress paths. The stresses along these paths are shown in Figure 3-12. These stress results are used in the crack growth evaluation.

Table 3-1: Component Materials

Component	Material
Reactor Pressure Vessel Shell	SA-533, Grade B, Class 1
Cladding	SA-182 F304
Recirculation inlet Nozzle	SA-508, Class 2
Nozzle Weld Butter	Alloy 82/182
Vessel-to-Nozzle Weld	SA-508, Class 2
Nozzle-to-Safe End DMW Weld	Alloy 82/182
ID Weld Repair	Alloy 82/182
Safe End	SA-182 F304
Safe End-to-Pipe Weld	Stainless Type 304
Attached Pipe	Stainless Type 304
Thermal Sleeve	SA-182 F304
Weld Overlay (WOL)	Alloy 52M

Table 3-2: Material Properties for SA-533, Grade B, Class 1 (Mn-1/2Mo/1/2Ni)

Temperature (°F)	E (x 10^6 psi)	Alpha (x 10^{-6} in/in/°F)	T_C (Btu/hr-ft-°F)	C (Btu/lb-°F)	σ_y (ksi)	σ_u (ksi)	ε_{total}
70	29.2	7.0	23.5	0.105	50.0	80.0	0.18
500	27.0	7.7	22.7	0.130	43.2	80.0	0.18 (6)
700	25.3	7.9	21.6	0.140	40.7	80.0	0.18 (6)
1100	17.8	8.3	19.0	0.173	24.0 (2)	56.0 (2)	0.30 (2)
1500	6.0 (2)	8.5	15.1	0.154	7.0 (2)	32.0 (2)	0.50 (2)
2500	0.1 (1)	9.0 (2)	5.0 (2)	0.204 (2)	1.0 (1)	2.0 (1)	0.99 (3)
2500.1	–	7.0 (7)	–	–	–	–	–

Notes:

(1) Negligible at high temperature and hence assumed a small value

(2) Estimated

(3) Molten metal at high temperature and hence assumed a large value

(4) Weight density is assumed to be temperature-independent at 0.283 lb/in^3

(5) Poisson's ratio is also assumed to be temperature-independent at 0.300

(6) Assumed proportional to σ_u

(7) Alpha at >2500.1°F is assigned value at 70°F to minimize fictitious thermal strain build-up

Table 3-3: Material Properties for SA-240, Type 304 Stainless (18Cr-8Ni)

Temperature (°F)	E (x 10^6 psi)	Alpha (x 10^{-6} in/in/°F)	T_C (Btu/hr-ft-°F)	C (Btu/lb-°F)	σ_y (ksi)	σ_u (ksi)	ε_{total}
70	28.3	8.5	8.6	0.116	35.0	90.0	0.60
500	25.8	9.7	10.9	0.131	22.0 (6)	69.0 (6)	0.48 (6)
700	24.8	10.0	11.8	0.135	20.0 (6)	67.0 (6)	0.45 (6)
1100	22.1	10.5	13.6	0.140	16.4 (6)	52.5 (6)	0.36 (6)
1500	18.1	10.8	15.3	0.145	13.0	23.0	0.46
2500	0.1 (1)	11.5 (2)	21.0 (2)	0.159 (2)	1.0 (1)	2.0 (1)	0.99 (3)
2500.1	–	8.5 (7)	–	–	–	–	–

Notes:
(1) Negligible at high temperature and hence assumed a small value
(2) Estimated
(3) Molten metal at high temperature and hence assumed a large value
(4) Weight density is assumed to be temperature-independent at 0.283 lb/in^3
(5) Poisson's ratio is also assumed to be temperature-independent at 0.300
(6) Interpolated
(7) Alpha at >2500.1°F is assigned value at 70°F to minimize fictitious thermal strain build-up

Table 3-4: Material Properties for SA-508 Grade 2 Class 1 (formerly SA-508 Class 2) (3/4Ni-1/2Mo-1/3Cr-V)

Temperature (°F)	E (x 10^6 psi)	Alpha (x 10^{-6} in/in/°F)	T_C (Btu/hr-ft-°F)	C (Btu/lb-°F)	σ_y (ksi)	σ_u (ksi)	ε_{total}
70	27.8	6.4	23.5	0.105	50.0	80.0	0.18
500	25.7	7.3	22.7	0.130	43.2	80.0	0.18 (6)
700	24.6	7.6	21.6	0.140	40.7	80.0	0.18 (6)
1100	21.5	8.2	19.0	0.173	24.0 (2)	56.0 (2)	0.30 (2)
1500	16.0 (2)	8.6 (2)	15.1	0.154	7.0 (2)	32.0 (2)	0.50 (2)
2500	0.1 (1)	9.5 (2)	5.0 (2)	0.204 (2)	1.0 (1)	2.0 (1)	0.99 (3)
2500.1	–	6.4 (7)	–	–	–	–	–

Notes:

(1) Negligible at high temperature and hence assumed a small value

(2) Estimated

(3) Molten metal at high temperature and hence assumed a large value

(4) Weight density is assumed to be temperature-independent at 0.283 lb/in^3

(5) Poisson's ratio is also assumed to be temperature-independent at 0.300

(6) Assumed proportional to σ_u

(7) Alpha at >2500.1°F is assigned value at 70°F to minimize fictitious thermal strain build-up

Table 3-5: Material Properties for Alloy 82/182/600 (N06600)

Temperature (°F)	E (x 10^6 psi)	Alpha (x 10^{-6} in/in/°F)	T_C (Btu/hr-ft-°F)	C (Btu/lb-°F)	σ_y (ksi)	σ_u (ksi)	ε_{total}
70	31.0	6.8	8.6	0.108	48.8	100.8	0.40
500	29.0	7.6	10.6	0.120	44.1	94.0	0.40
700	28.2	7.9	11.6	0.125	42.9	91.7	0.41
1100	25.9	8.4	13.8	0.139	40.4	73.0	0.40
1500	23.1	9.0	16.0	0.148	21.4	30.0	0.62
2500	0.1 (1)	10.0 (2)	22.0 (2)	0.177 (2)	1.0 (1)	2.0 (1)	0.99 (3)
2500.1	–	6.8 (7)	–	–	–	–	–

Notes:
(1) Negligible at high temperature and hence assumed a small value
(2) Estimated
(3) Molten metal at high temperature and hence assumed a large value
(4) Weight density is assumed to be temperature-independent at 0.300 lb/in^3
(5) Poisson's ratio is also assumed to be temperature-independent at 0.290
(7) Alpha at >2500.1°F is assigned value at 70°F to minimize fictitious thermal strain build-up

Table 3-6: Material Properties for Alloy 52/52M/52MS/690 (N06690)

Temperature (°F)	E (x 10^6 psi)	Alpha (x 10^{-6} in/in/°F)	T_C (Btu/hr-ft-°F)	C (Btu/lb-°F)	σ_y (ksi)	σ_u (ksi)	ε_{total}
70	30.3	7.7	6.8	0.107	48.7	100.3	0.49
500	28.3	8.1	9.4	0.121	36.5	86.7	0.44
700	27.6	8.3	10.6	0.125	34.5	85.7	0.43
1100	25.3	8.5 (2)	13.1	0.135	31.7	72.0	0.47
1500	22.6	8.8 (2)	15.5	0.147	28.1	40.6	0.91
2500	0.1 (1)	9.5 (2)	22.0 (2)	0.167 (2)	1.0 (1)	2.0 (1)	0.99 (3)

Notes:

(1) Negligible at high temperature and hence assumed a small value

(2) Estimated

(3) Molten metal at high temperature and hence assumed a large value

(4) Weight density is assumed to be temperature-independent at 0.293 lb/in^3

(5) Poisson's ratio is also assumed to be temperature-independent at 0.290

Table 3-7: Yield Strength and Ultimate Strength

Material	Temperature (°F)	Yield Strength (ksi)	Ultimate Strength (ksi)	ε_{total}
SA-533 Grade B Class 1	70	50.0	80.0	0.18
	500	43.2	80.0	0.18
	700	40.7	80.0	0.18
	1100	24.0	56.0	0.30
	1500	7.0	32.0	0.50
	2500	1.0	2.0	0.99
Type 304 Stainless	70	35.0	90.0	0.60
	500	22.0	69.0	0.48
	700	20.0	67.0	0.45
	1100	16.4	52.5	0.36
	1500	13.0	23.0	0.46
	2500	1.0	2.0	0.99
SA-508 Class 2	70	50.0	80.0	0.18
	500	43.2	80.0	0.18
	700	40.7	80.0	0.18
	1100	24.0	56.0	0.30
	1500	7.0	32.0	0.50
	2500	1.0	2.0	0.99
Alloy 82/182	70	54.5	98.1	0.45
	500	47.5	86.8	0.45
	700	46.8	84.5	0.45
	1100	45.0	76.6	0.45
	1500	29.8	40.8	0.67
	2500	1.0	2.0	0.99
Alloy 600	70	48.8	100.8	0.40
	500	44.1	94.0	0.40
	700	42.9	91.7	0.41
	1100	40.4	73.0	0.40
	1500	21.4	30.0	0.62
	2500	1.0	2.0	0.99
Alloy 52M	70	48.7	100.3	0.49
	500	36.5	86.7	0.44
	700	34.5	85.7	0.43
	1100	31.7	72.0	0.47
	1500	28.1	40.6	0.91
	2500	1.0	2.0	0.99

Table 3-8: Assumed Heat Input for ID Repair Welding

Parameter	Value
Weld bead width	0.25 in
Weld bead thickness	0.10 in
Nugget Heat Input	28 kJ/in
Heat efficiency	0.70
Heat Input Cycle	12 sec.

Table 3-9: Assumed Heat Input for Weld Overlay Welding

Parameter	Value
Weld bead width	0.25 in
Weld bead thickness	0.10 in
Nugget Heat Input	35 kJ/in
Heat efficiency	0.70
Heat Input Cycle	12 sec.

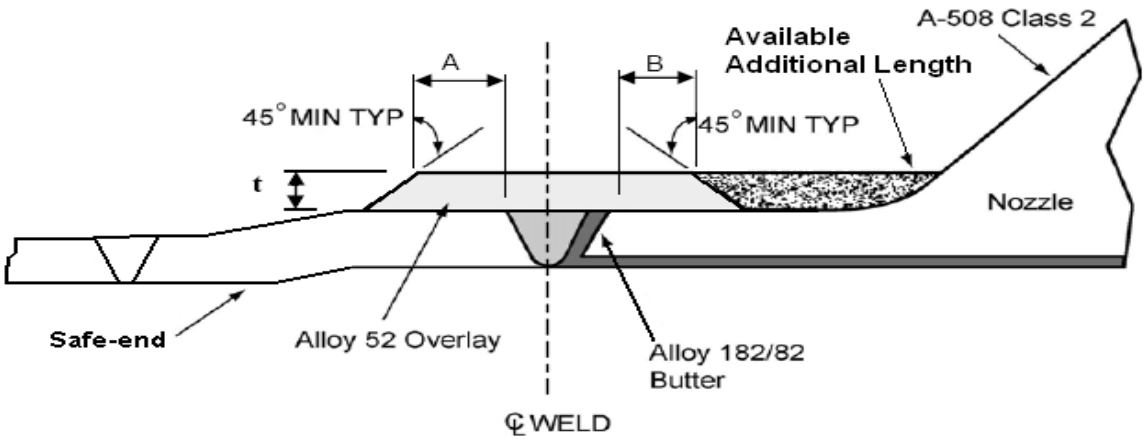

WELD NUMBER	FLAW CHARACTERIZATION	DESIGN DIMENSIONS			COMMENTS
		t	A	B	
Nozzle N2G Recirc. Inlet Weld Overlay	Assumed 360° Circ. 100% through wall flaw	0.432" (Note 3) (Note 4)	1.732" min.	1.737" min. (Note 7)	A is measured from the DM weld-safe-end interface; B is measured from the butter-nozzle interface

0	CJF 02/26/10	AJG 02/26/10	GAM 02/26/10	
Revision	Prepared by/Date	Checked By/Date	Approved by/Date	COMMENTS

Job No: 0900556.00	Plant/Unit:	STRUCTURAL INTEGRITY ASSOCIATES, INC.
File No: 0900556.501	Hatch Unit 2	
Drawing No: 0900556.501	Title: Standard Weld Overlay Design	Sheet 1 of 2

NOTES

1. Prior to deposition of the weld overlay, the surface to be repaired shall be examined by the liquid penetrant method. Indications larger than 1/16 in. (1.5 mm) shall be removed, reduced in size, or corrected in accordance with the following requirements.

    i. One or more layers of weld metal shall be applied to seal unacceptable indications in the area to be repaired with or without excavation. The thickness of these layers shall not be used in meeting weld reinforcement design thickness requirements. Peening the unacceptable indication prior to welding is permitted.
    ii. If correction of indications identified above is required, the area where the weld overlay is to be deposited, including any local repairs or initial weld overlay layer, shall be examined by the liquid penetrant method. The area shall contain no indications greater than 1/16 in. (1.5 mm) prior to the application of the structural layers of the weld overlay.

2. Weld overlay wire shall be ERNiCrFe-7A (Alloy 52M).

3. The minimum design thickness, t (0.432 inches), is the minimum thickness beyond the first clean surface or layer.

4. Apply as many layers as required to achieve the design overlay thickness "t".

5. Design thickness includes no allowance for surface conditioning operations to facilitate UT inspection.

6. Length shown includes the minimum required for structural reinforcement plus additional length for UT inspection; greater length may be required for effective UT inspection. This is to be determined in the field.

7. Overlay to be blended gently into nozzle to minimize stress concentration and to accommodate temper bead weld passes. Extra temper bead may be applied approximately 1/8" above the blend to facilitate additional layers if necessary.

Job No: 0900556.00	**Plant/Unit:**	STRUCTURAL INTEGRITY ASSOCIATES, INC.	
File No: 0900556.501	**Hatch Unit 2**		
Drawing No: 0900556.501	**Title: Standard Weld Overlay Design**		**Sheet 2 of 2**

Figure 3-1: Weld Overlay Design

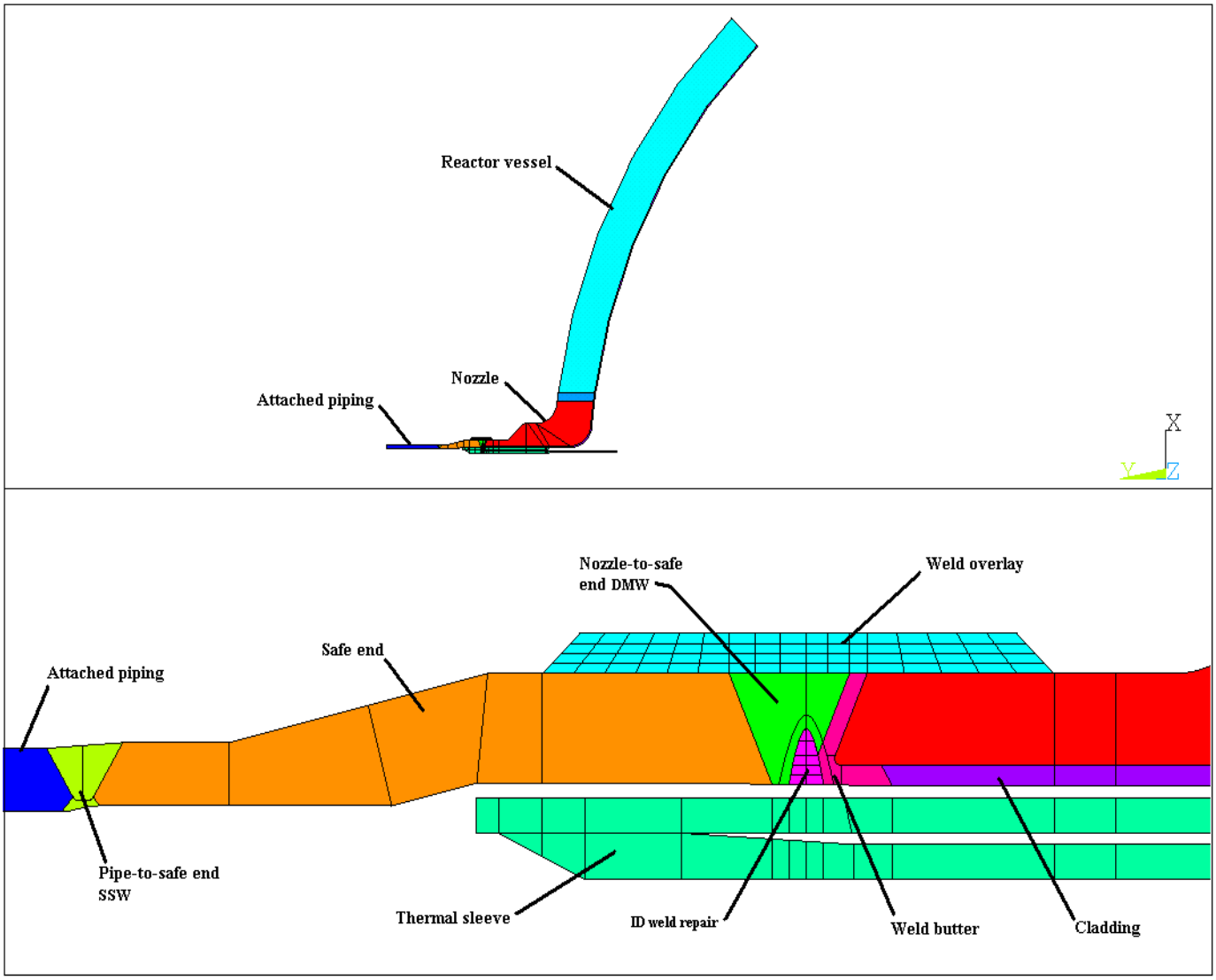

Figure 3-2: As-Modeled Component Definitions

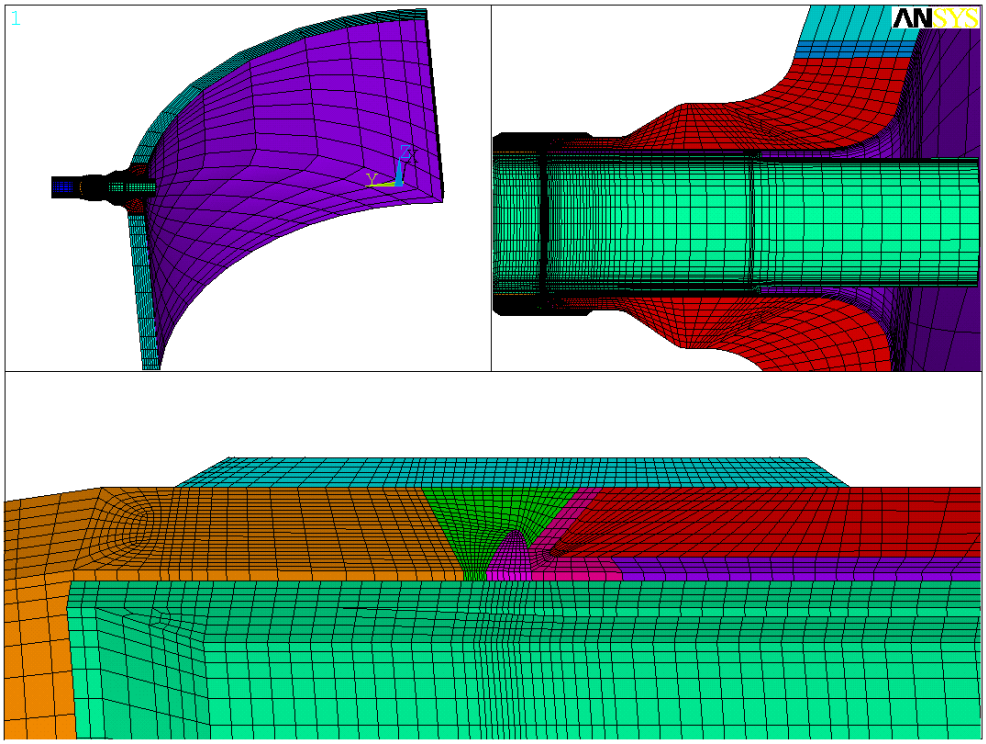

a) 3-D Finite Element Model

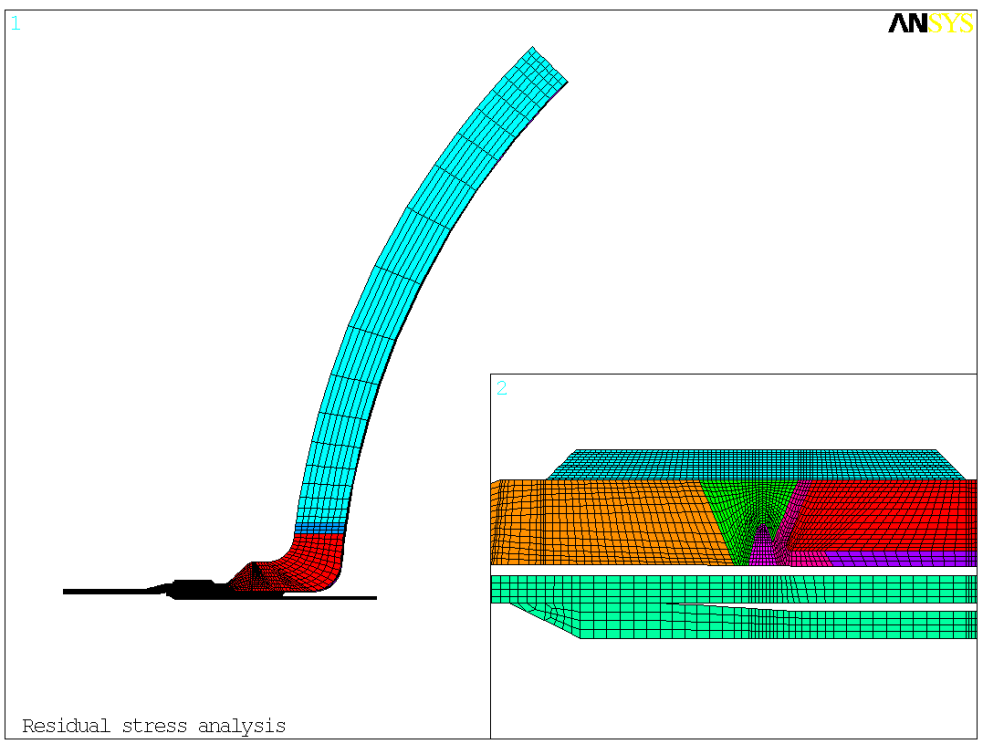

b) 2-D Finite Element Model

Figure 3-3: Finite Element Model of Recirculation Inlet Nozzle

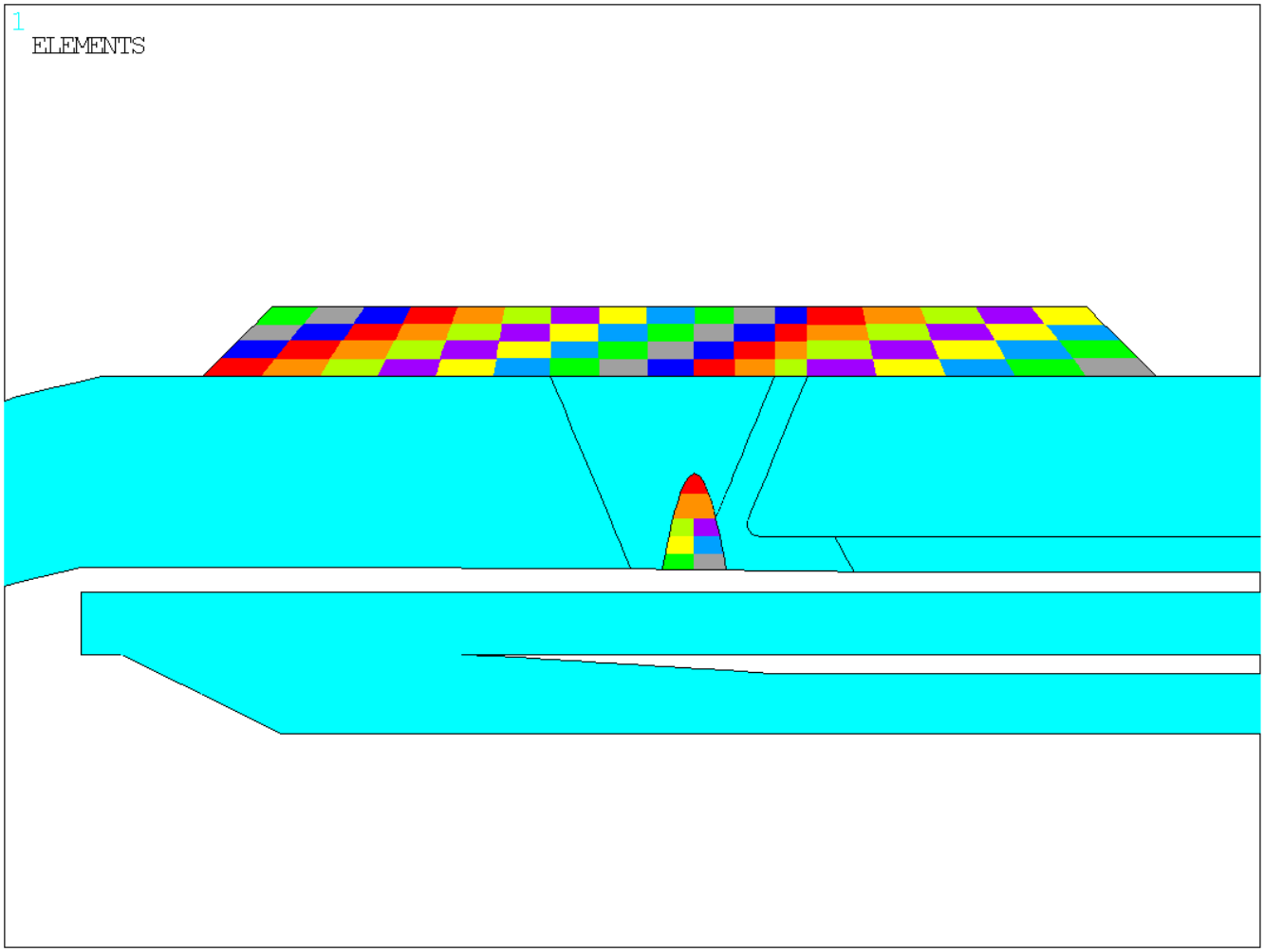

Figure 3-4: As-Modeled Nuggets for ID Weld Repair and Weld Overlay

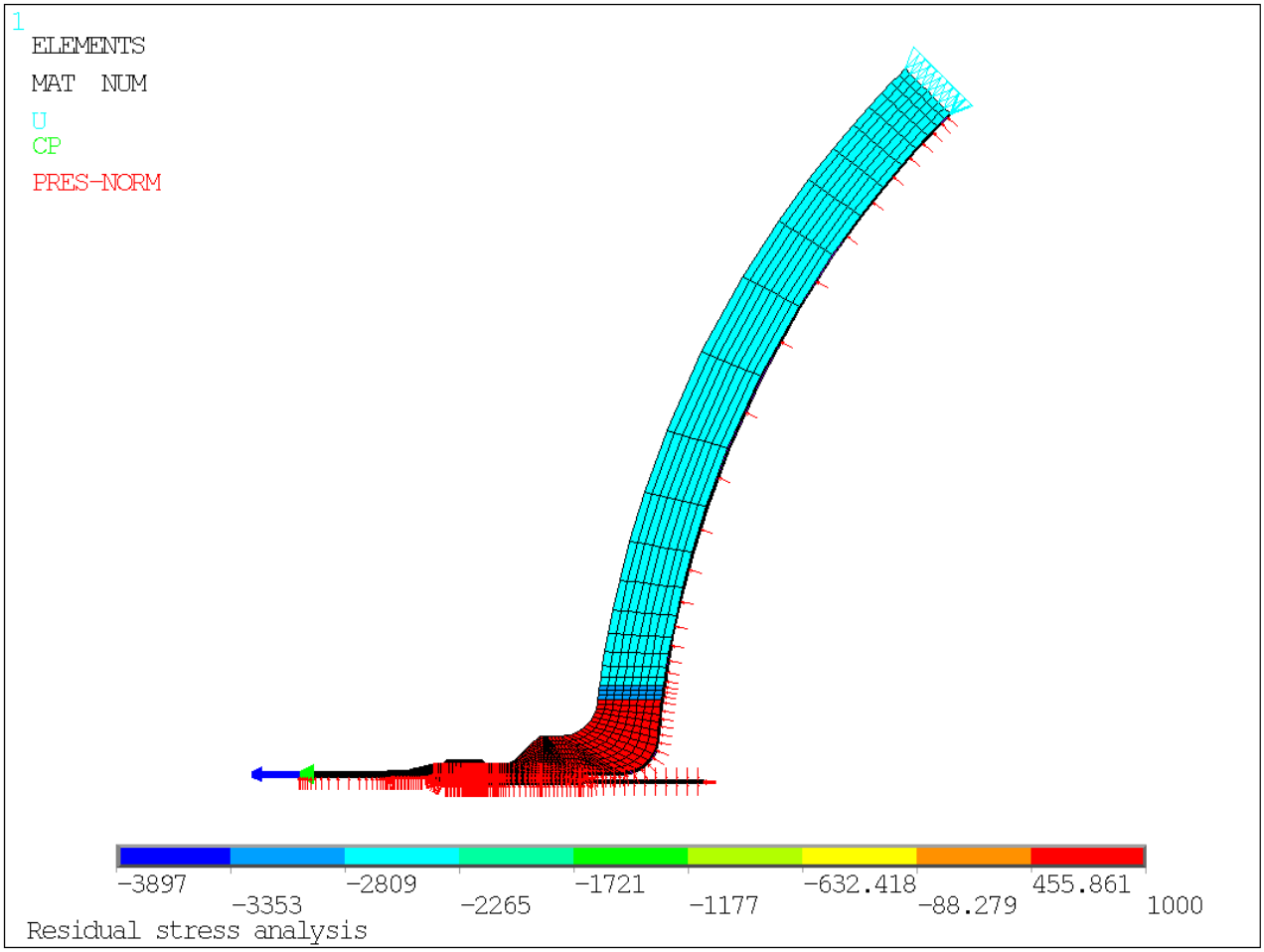

Figure 3-5: Applied Boundary Conditions to the Finite Element Model

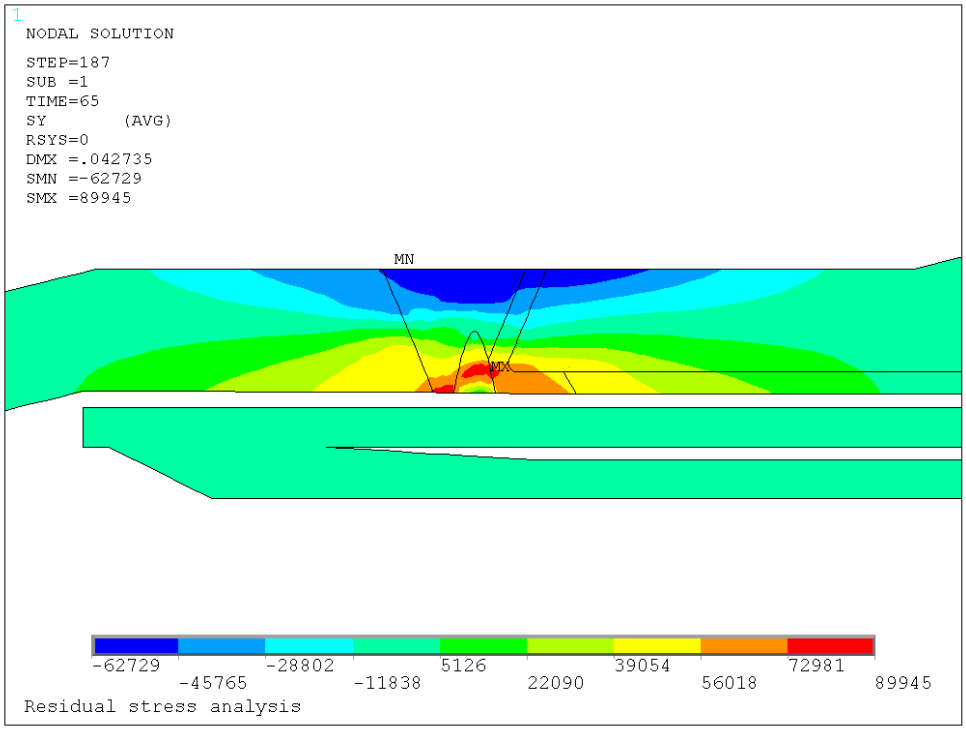

a) Axial Stress (psi)

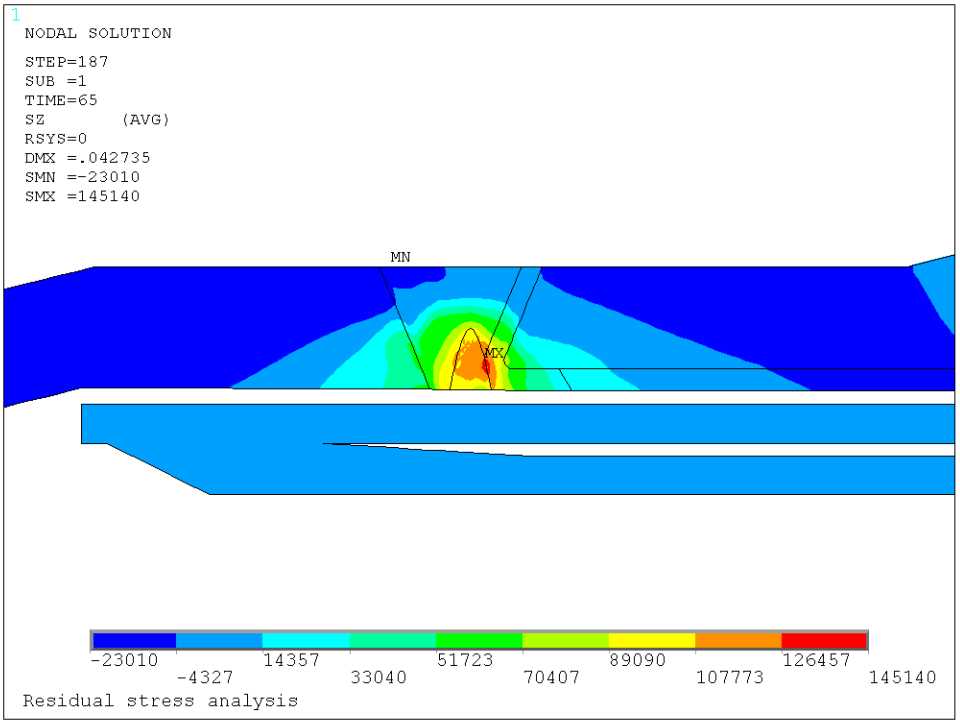

b) Hoop Stress (psi)

Figure 3-6: ID Weld Repair Residual Stresses

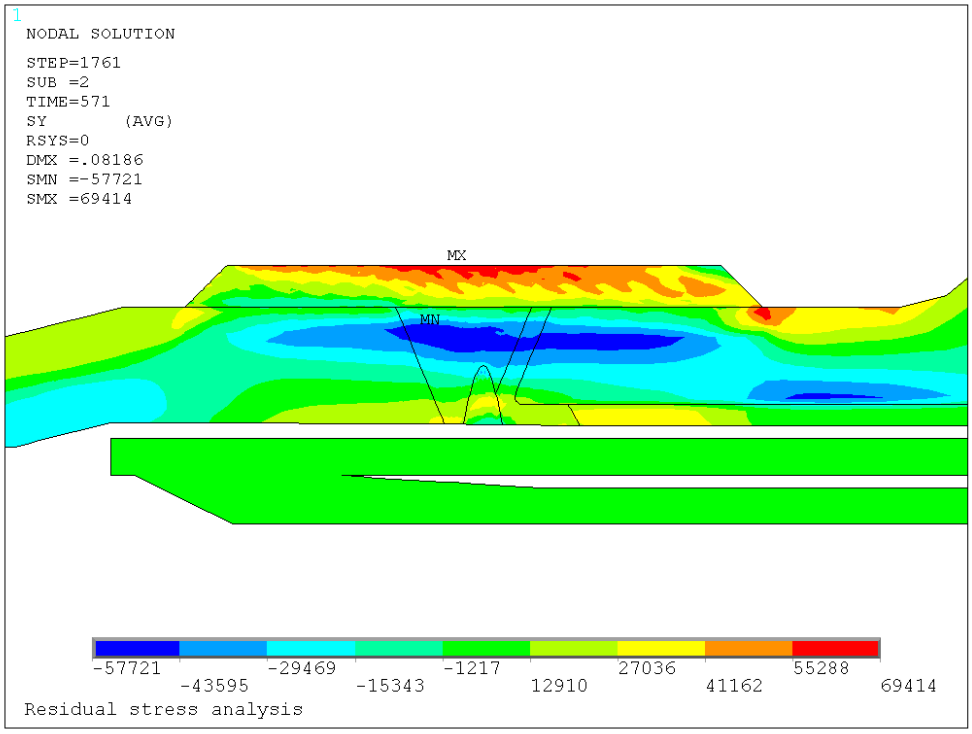

a) Axial Stress (psi)

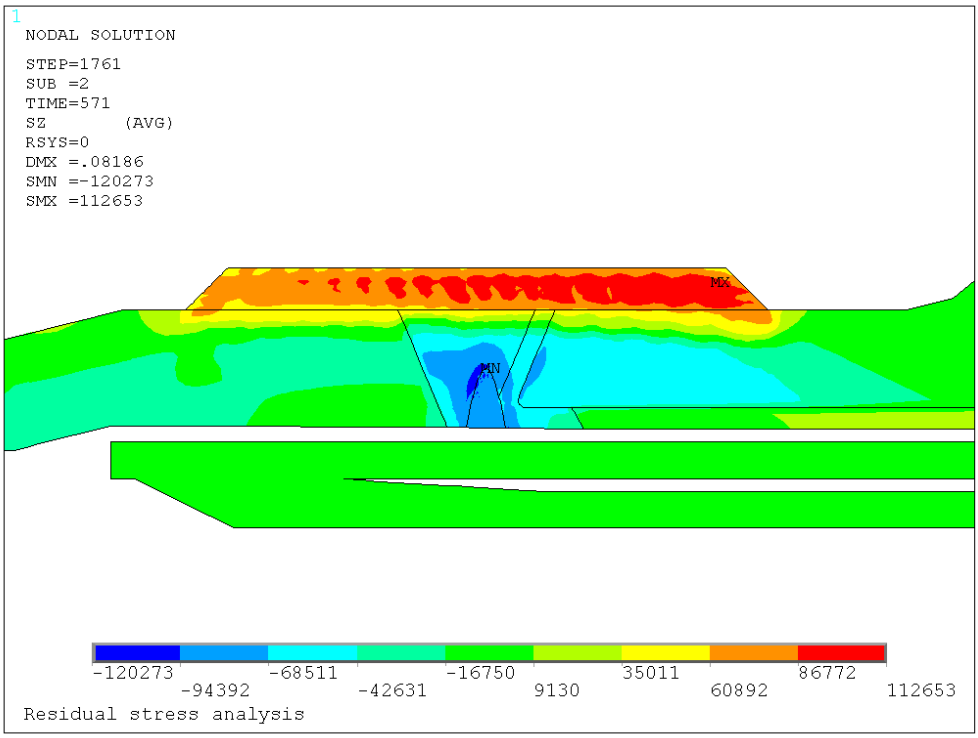

b) Hoop Stress (psi)

Figure 3-7: Weld Overlay Residual Stresses at 70°F

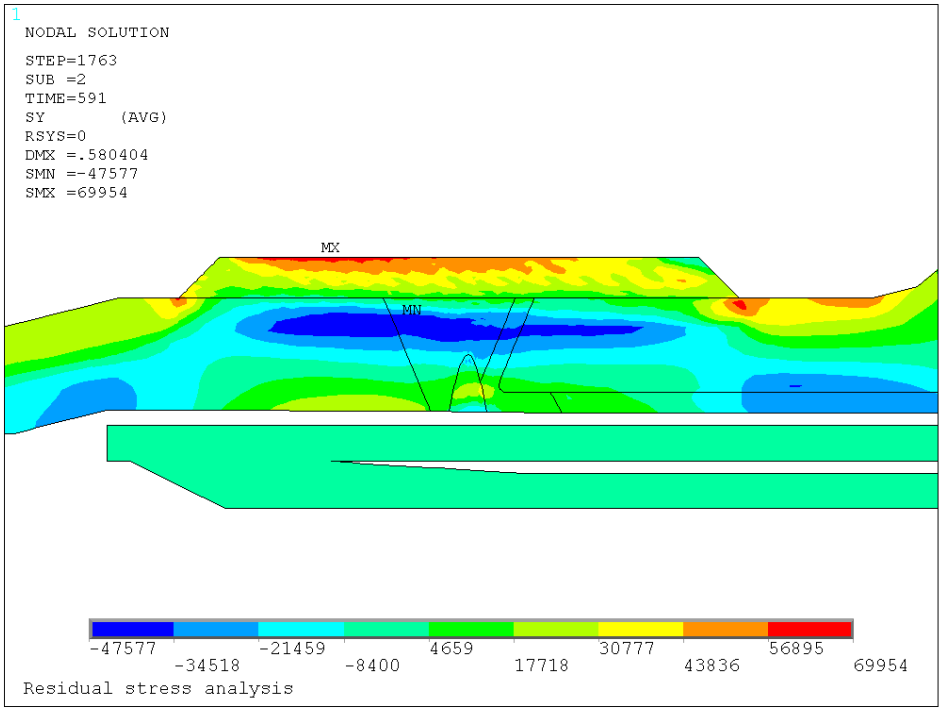

a) Axial Stress (psi)

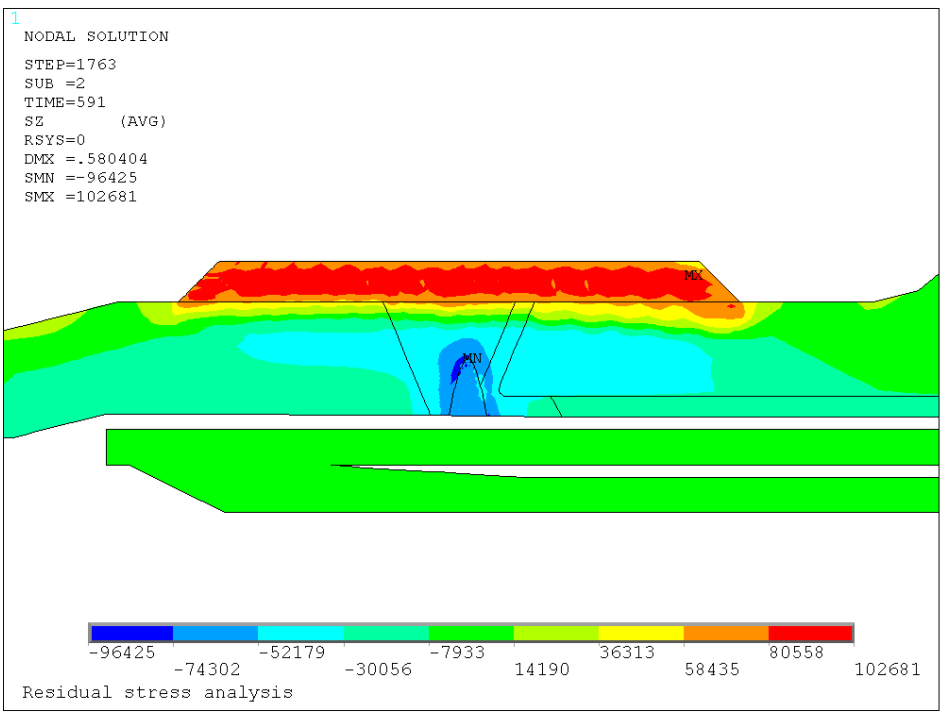

b) Hoop Stress (psi)

Figure 3-8: Weld Overlay Stresses at 546°F and 1000 psia

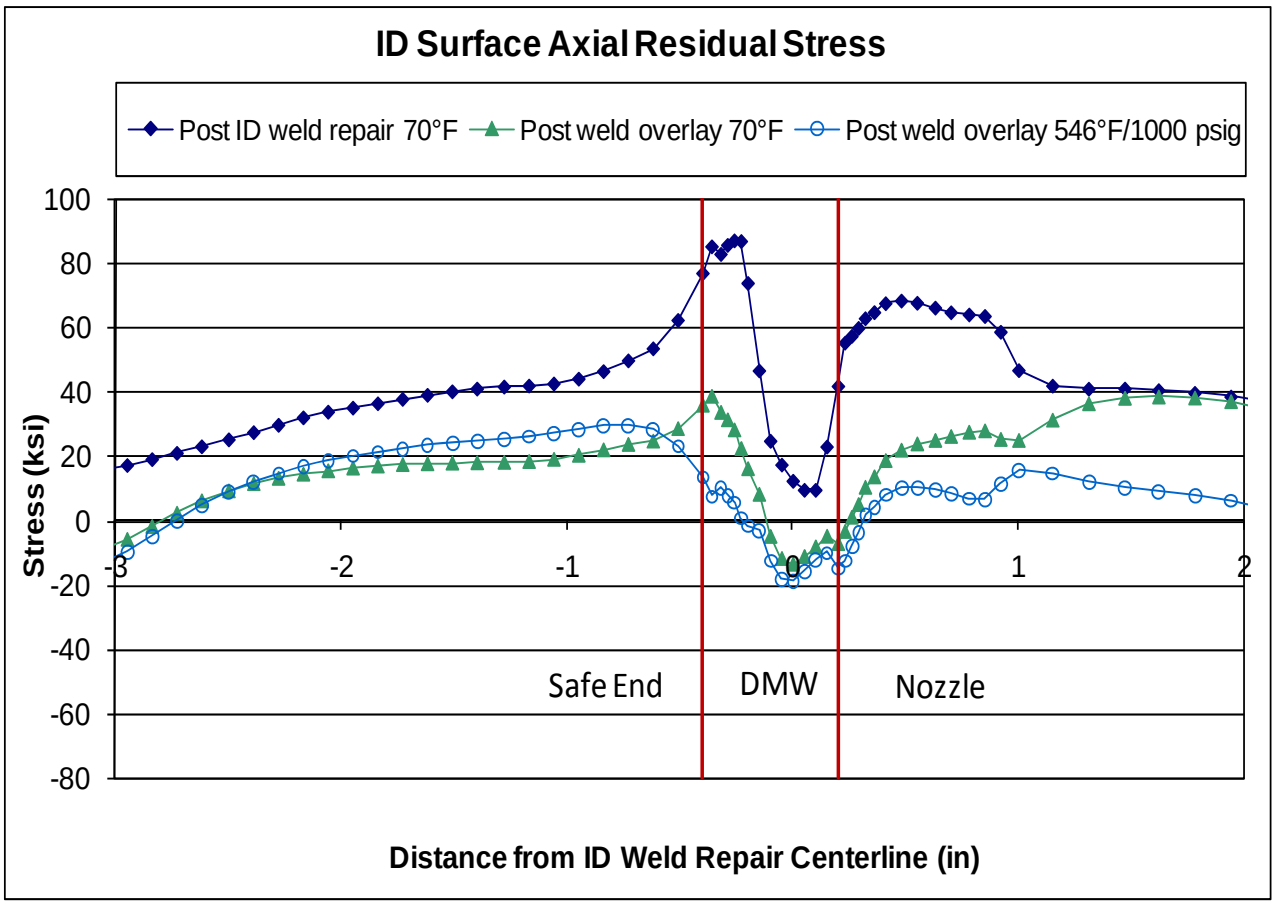

Figure 3-9: ID Surface Axial Stresses

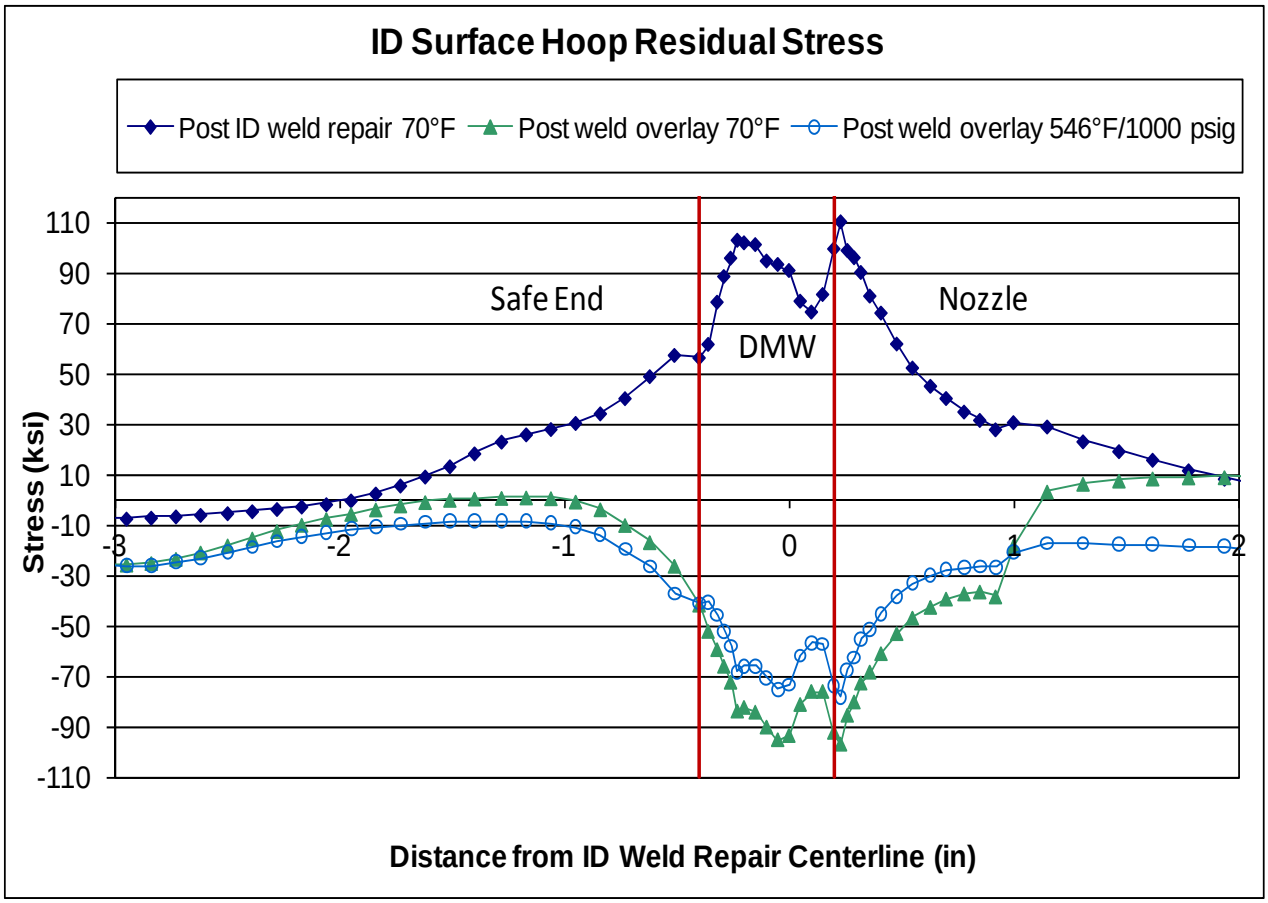

Figure 3-10: ID Surface Hoop Stresses

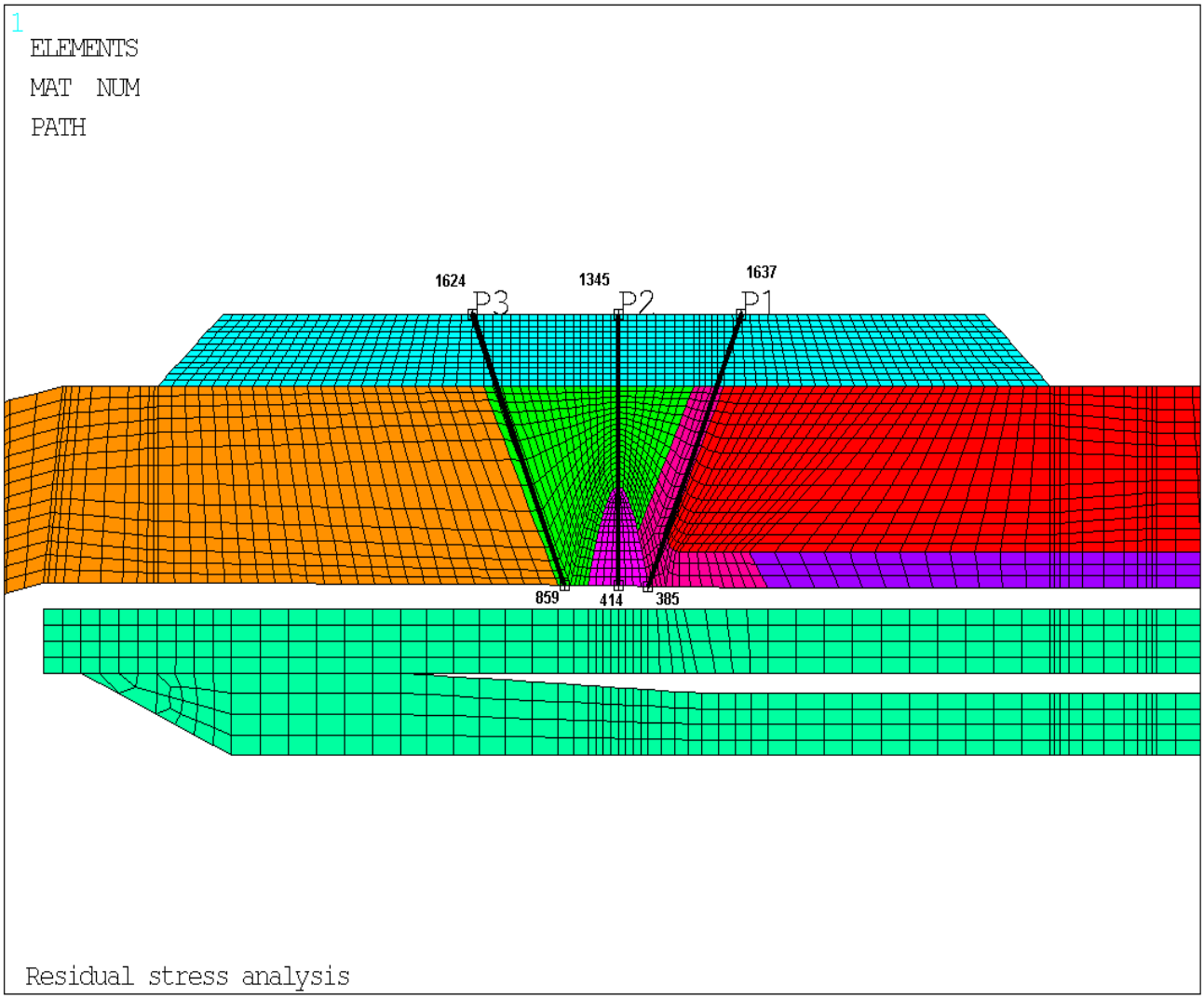

Figure 3-11: Stress Path Definitions

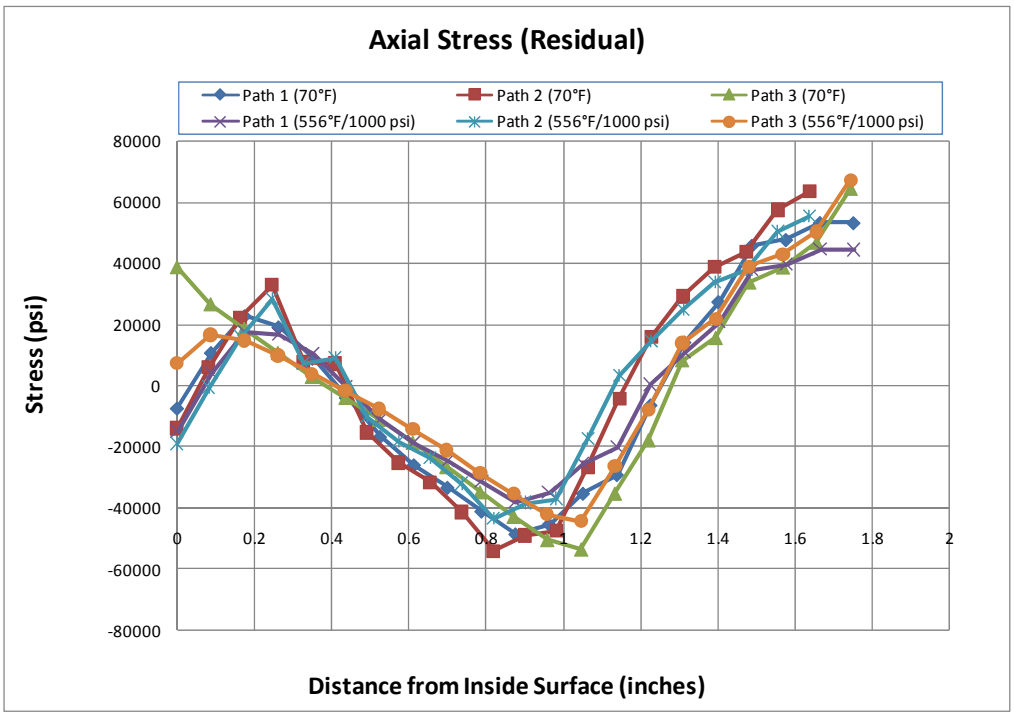

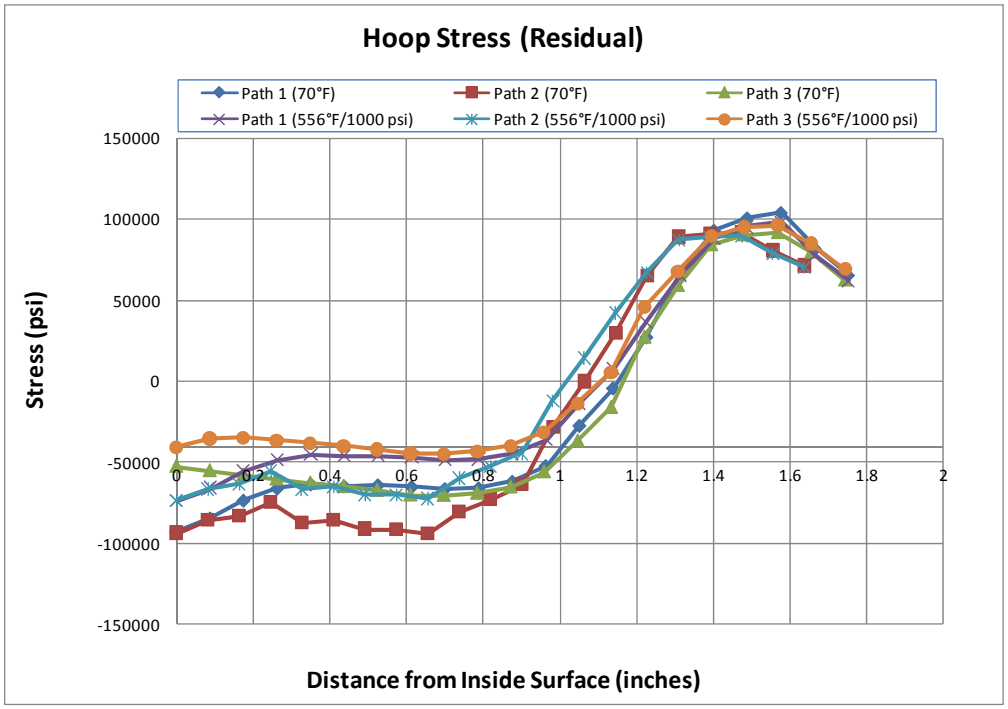

Figure 3-12: Through-Wall Residual Stress Path Profiles

4.0 EVALUATION OF WELD OVERLAY SHRINKAGE STRESSES

ISI-ALT-08-02 [3] also requires that the impact of the weld overlay on the attached piping system and supports be addressed. Stresses develop in a piping system after application of one or more weld overlays due to the weld shrinkage at the overlays caused by the restraint and stiffness of the attached piping. These stresses are system-wide, and are similar in nature to restrained free-end thermal expansion or contraction stresses. The level of stresses resulting from weld overlay shrinkage is a direct result of the number and location of the weld overlays, the shrinkage per overlay, and the piping system geometry. Axial shrinkage produces tensile stresses at locations co-linear with the overlay, and predominantly bending stresses at locations which are separated and not co-linear with the welding location.

The stresses due to weld overlay shrinkage will be addressed in a reconciliation report following implementation of the overlay.

5.0 ASME CODE STRESS EVALUATION

5.1 Background

This section presents the discussion of the ASME Code Section III [13] evaluation for the weld overlay. ISI-ALT-08-02 [3] requires that the overlay be sized so that it will be able to provide for load redistribution from the pipe into the deposited weld metal and back into the pipe without violating applicable stress limits of ASME Code, Section III for primary, secondary, and peak stresses. The ASME Code stress evaluation is documented in detail in Reference 14.

5.2 Technical Approach

A three-dimensional finite element model is used in the stress analyses for this evaluation. The model, which is described in detail in Reference 12, included a portion of the reactor vessel and all components out to the recirculation inlet piping. The DMW region was modeled in detail since it is the area of most interest.

Static and transient analyses are performed for internal pressure and thermal transients to determine the appropriate stresses. The resulting stresses are compared to determine the impact of the repair on ASME Code Section III allowable stresses and fatigue usage.

The temperature-dependent material property values are presented in Section 3.0. The same boundary conditions previously identified in Section 3.0 will also be used for all subsequent evaluations in this section.

Weld residual stresses resulting from the original welding of the various components, the postulated weld repair and the weld overlay are not considered here as they are not required for ASME Code, Section III stress evaluations.

The thermal transients and operating pressure loads are provided in Reference 12.

5.3 Analysis

The following loads were considered in the design of the weld overlay repair.

Pressure

The design pressure of the vessel coolant and nozzle flow path is given as 1,250 psig and 1,423 psig, respectively [10, A-671]. For the thermal transients applicable to the recirculation inlet nozzle, the pressures range between zero and the normal operating pressure (1,000 psig) [10]. The maximum design pressure of 1,423 psig was conservatively used for the ASME Code Section III primary stress evaluation.

Thermal Transients

The four bounding thermal transients for the recirculation inlet nozzle and are evaluated to obtain thermal stress results in Reference 12. The bounding transients are summarized as follows:

Description	Time, sec	Vessel Temp, °F	Nozzle Temp, °F
Startup	0	100	100
Transient ID No. 1	16056	546	546
Shutdown	0	546	546
Transient ID No. 2	6156	375	375
	6156	375	300
	6756	330	260
	12516	170	100
	15036	100	100
Scram	0	522	522
Transient ID No. 3	4392	400	400
	9648	546	546
Loss of AC Power	0	522	522
Transient ID No. 4	220	300	300
	2200	500	500
	2380	300	300
	6760	500	500
	7180	300	300
	10180 (steady)	300	300
	19036	546	546
	22636	546	546
	22636	538	538
	24436	522	522

Mechanical Piping Loads

The recirculation inlet nozzle is subjected to a number of mechanical piping loads. Per Table 1 in Reference 1, the mechanical piping loads for the nozzle are reported in Table 5-1. The thermal sleeve loads acting on the nozzle are small and subsequently are not considered. Note that Table 5-1 also shows piping loads for the deadweight condition. However, deadweight loads are constant loads which occur for all load conditions. Therefore, deadweight loads do not contribute to the stress ranges for Service Levels A and B load combinations and fatigue evaluations (per NB-3222.2 and NB-3222.4 for vessels and NB-3653.1, NB-3653.2 and NB-3653.5 for piping), and therefore do not need to be included. The deadweight loads were conservatively included, however, as shown in Table 5-1. The resultant piping moments of 863,646 in-lbs and 1,382,839 in-lbs were used for the Level A/B and Level C/D Code evaluations, respectively.

5.4 Load Combinations

The different service levels are evaluated as follows:

Service Level A/B: Design Pressure + Deadweight + Thermal + OBE
Service Level C/D: Design Pressure + Deadweight + Thermal + SSE

The allowable stress intensities are presented in Table 5-2.

5.5 ASME Code Section III Evaluation

Stress intensities are calculated for the load combinations mentioned above, and compared to the allowable limits shown in Table 5-2. Using the ANSYS [8] output results for unit load cases and thermal transients, reported in Reference 12, linearized through-wall stresses were evaluated for all paths, as shown in Figure 5-1, for the pressure and mechanical load analyses and the thermal transients. These calculated stress intensities are then evaluated in accordance with ASME Code, Section III, Subarticle NB-3200 [13] with guidance from Subarticle NB-3600 [13] for each path location.

Table 5-2 shows the ASME Code design stress intensities considered for each material for the recirculation inlet nozzle assembly.

For the Code stress evaluation (Subparagraphs NB-3653.1 and NB-3653.2 [13]) of stress intensity range, examination of the membrane-plus-bending stresses from Reference 12 does not provide an obvious pairing of stresses resulting from the various thermal transients for determination of operating ranges. Therefore, the range is conservatively taken as the sum of the largest two thermal transient stress results.

The results of the Code stress evaluation for P_m and $P_L + P_b$ for the different paths are given in Tables 5-3 and 5-4 which correspond to Service Levels A/B and C/D, respectively. From Table 5-3 it is shown that the P_m and P_L+P_b in all the stress paths are below the Level A/B Service condition allowable stress intensities. From Table 5-4 it is shown that the P_L and P_L+P_b in all the stress path locations are below the Level C/D Service condition allowable stress intensities.

5.5.1 Fatigue Evaluation

The fatigue evaluations are performed for all paths taken at the weld overlay repair (see Figure 5-1). Both the inside and outside edges of the indicated paths are evaluated. The evaluations are performed in accordance with ASME Code, Section III, Subparagraph NB-3222.4(e) [13], using guidance from Subarticle NB-3600.

The total number of design cycles for each bounding event is tabulated in Table 5-5. The materials at the inside and outside surfaces of the stress paths are tabulated in Table 5-6.

The fatigue cycles shown in Table 5-5 are grouped as follows; it should be noted that, since the Blowdown transient and Loss of Feedwater transient are not specified in the Design Report [10] for the recirculation inlet nozzle, these transient events and seismic cycles have been grouped with the Loss of A.C. Power transient, which has the highest stress results.

Startup/Shutdown:	120 cycles
Design Pressure Test:	130 cycles

Scram:	180 cycles
LOP:	115 x (3 internal cycles) = 345 cycles (includes 15 LOP cycles, 10 blowdown, 10 seismic, and 80 Loss of Feedwater cycles)

These fatigue cycles are distributed evenly over 40 years. The membrane-plus-bending-plus-peak (P+Q+F) component stresses from Table 5-3 (Service Level A/B conditions) are used for determination of the alternating stress, $S_a = (P+Q+F)/2$. The fatigue usage is calculated for each stress path location using the alternating stress and the bounding fatigue curves shown in Figure 5-2, which are given in the ASME Code [2], based on the bounding material at each path location.

5.6 Results of Analysis

5.6.1 ASME Code, Section III Evaluation

The results in Table 5-3 and Table 5-4 show that Primary-plus-Secondary stresses are below the ASME code allowable stresses. All stresses were below the maximum allowable values.

5.6.2 Fatigue Evaluation

The allowable cycles at each path are obtained based on the peak stresses (P_L+P_B+Q+F) presented in Table 5-3 for the Service Level A/B conditions. As reported in Table 5-7, the highest fatigue usage is 0.105 at Path 14 (at the toe of the weld overlay).

In addition, for comparison, a fatigue strength reduction factor of 1.8 per NB-3680 for taper transitions is used to multiply the P_L+P_B+Q to obtain the P_L+P_B+Q+F stress category for fatigue usage evaluation. The results are presented in Table 5-8. The resulting fatigue usage factor is 0.154 at the Path 14 location.

5.6.3 Extended Power Uprate (EPU) Considerations

Note that the transient conditions evaluated in Reference 12 do not include extended power uprate (EPU) conditions. Rather, the thermal, pressure, and mechanical loadings, used to determine the stress and fatigue results reported therein, were based on original plant design conditions. Therefore, the results were factored to account for EPU. The EPU task report [20]

documents an increase in pressure from 1,000 psig to 1,048 psig, which is an increase of 4.8%. The report also documents increases in temperature for the reactor vessel Regions A, B, and C. Of the revised temperatures shown, the largest increase is from 435°F to 441°F, which is an increase of approximately 1.6% in Region B where the recirculation nozzle is located. Since the detailed stress and fatigue calculations [14] were performed using the design pressure of 1,423 psi (rather than the operating pressure), no additional factors were added to the pressure stress results. The stress and fatigue results were increased by 1.6% to account for increases in thermal stress.

For Service Level A/B loads, the bounding P_m stress increased from 12.92 ksi (Path 5) to 13.13 ksi, compared to an allowable value of S_m = 16.60 ksi (see Table 5-3). The bounding P_L+P_b stress increased from 16.29 ksi (Path 5, inside location) to 16.55 ksi, compared to the allowable value of $1.5S_m$ = 24.90 ksi. Likewise, the bounding P_L+P_b+Q stress increased from 68.37 ksi (Path 3, inside location) to 69.46 ksi, compared to an allowable value of $3S_m$ = 69.90 ksi.

For Service Level C/D loads, the bounding P_m stress increased from 16.37 ksi (Path 5) to 16.63 ksi, compared to an allowable value of $1.2S_m$ = 19.92 ksi (see Table 5-4). The bounding P_L+P_b stress increased from 20.00 ksi (Path 5, inside location) to 20.32 ksi, compared to the allowable value of $1.8S_m$ = 29.88 ksi.

The bounding fatigue usage was 0.154 at Path 14 (Table 5-8), and therefore an increase of 1.6% in thermal stresses will result in a fatigue usage of 0.156.

5.7 Concluding Remarks – Stress Evaluation

An evaluation has been performed to determine the impact of the weld overlay repair of the Hatch, Unit 2, recirculation inlet nozzle dissimilar metal weld N2G, based on ASME Code, Section III rules. The evaluation included primary-plus-secondary Code acceptance and fatigue usage calculations. It was determined that the impact is minor and generally produces a more favorable stress condition, and fatigue is not significant for the balance of plant life.

Table 5-1: Attached Piping Loads

				At pipe-to-safe-end weld			At nozzle-to-safe-end weld			
	Forces (kips)			Moments (in-kips)			Moments (in-kips)			
	Fx (axial)	Fy	Fz	Mx (axial)	My	Mz	Mx (axial)	My	Mz	SRSS (in-lbs)
Deadweight	0.00	6.67	6.67	0.00	180.20	180.20	0.00	243.57	243.57	NA
OBE	0.00	13.35	13.35	0.00	240.30	240.30	0.00	367.13	367.13	NA
DBE	0.00	26.70	26.70	0.00	480.60	480.60	0.00	734.25	734.25	NA
Total (Level A)	0.00	6.67	6.67	0.00	180.20	180.20	0.00	243.57	243.57	344,453
Total (Level B)	0.00	20.02	20.02	0.00	420.50	420.50	0.00	610.69	610.69	863,646
Total (Level C)	0.00	33.37	33.37	0.00	660.80	660.80	0.00	977.82	977.82	1,382,839
Total (Level D)	0.00	33.37	33.37	0.00	660.80	660.80	0.00	977.82	977.82	1,382,839

Note: Reproduced from Reference 1

Table 5-2: Summary of Stress Intensity Limits

Component	Material [1]	Level A/B Allowable Stress Intensity (ksi)		
		S_m (P_m)	$1.5S_m$ (P_L+P_B)	$3S_m$ (P_L+P_B+Q)
Reactor Vessel	SA-533 Grade B, Class1	26.7	40.05	80.1
Nozzle Forging	SA-508 Class 2	30.0	45.0	90.0
Cladding	SA-182 F304	16.6	24.9	49.8
Safe End	SA-182 F304	16.6	24.9	49.8
Weld/Repair/Butter	Alloy 82/182 (Alloy 600)	23.3	34.95	69.9
Overlay	Alloy 52M	23.3	34.95	69.9

Categories	Levels A and B (Design, Normal, & Upset)	Level C/D (Emergency/Faulted)
P_L	Sm	Min. of $1.2S_m$ and S_y
P_L+P_B	1.5Sm	Min. of $1.8S_m$ and $1.5S_y$
P_L+P_B+Q	3Sm[(a)]	n/a
P_L+P_B+Q+F	Note (a)	n/a

Notes:

n/a : not applicable

a. The requirements of ASME Code, Section III, Subparagraph NB-3222.4(e) along with Subparagraph NB-3653.5 [13], for peak stresses and cyclic operation must be met.

Table 5-3: Code Stress Evaluation for Service Level A/B Loads

Path	Material	P_m (ksi)	S_m (ksi)	P_L+P_B (ksi)	$1.5S_m$ (ksi)	$P_L+P_B+Q^3$ (ksi)	$3S_m$ (ksi)	P_L+P_B+Q+F (ksi)
Inside Path Location								
1	Alloy 182	10.03	23.30	12.54	34.95	56.28	69.90	69.06
2	Alloy 182	10.36	23.30	12.91	34.95	54.75	69.90	65.88
3	Alloy 182	10.73	23.30	13.59	34.95	68.37	69.90	82.46
4	SA-182, F304	8.88	16.60	8.62	24.90	40.42	49.80	60.38
5	SA-182, F304	12.92	16.60	16.29	24.90	39.29	49.80	52.50
11	Alloy 182	9.50	23.30	10.91	34.95	55.32	69.90	67.83
12	Alloy 182	9.73	23.30	10.91	34.95	53.43	69.90	64.37
13	Alloy 182	10.01	23.30	11.16	34.95	66.08	69.90	80.02
14	SA-182, F304	9.25	16.60	9.33	24.90	40.71	49.80	61.57
15	SA-182, F304	11.70	16.60	12.86	24.90	35.87	49.80	48.76
Outside Path Location								
1	Alloy 182/52M	10.03	23.30	7.54	34.95	29.71	69.90	38.05
2	Alloy 182/52M	10.36	23.30	7.84	34.95	27.34	69.90	33.78
3	Alloy 182/52M	10.73	23.30	7.93	34.95	51.07	69.90	69.51
4	SA-508 / Alloy 52M	8.88	23.30	9.74	34.95	49.63	69.90	76.37
5	SA-182, F304 / Alloy 52M	12.92	16.60	9.92	24.90	40.68	49.80	74.11
11	Alloy 182/52M	9.50	23.30	8.09	34.95	30.73	69.90	38.89
12	Alloy 182/52M	9.73	23.30	8.55	34.95	28.53	69.90	34.86
13	Alloy 182/52M	10.01	23.30	8.87	34.95	51.91	69.90	70.28
14	SA-508 / Alloy 52M	9.25	23.30	13.24	34.95	53.18	69.90	84.15
15	SA-182, F304 / Alloy 52M	11.70	16.60	10.91	24.90	41.99	49.80	76.36

Notes:

1. All units are in ksi
2. The P_m and P_L for Pressure load case are conservatively scaled to 1,423 psi design pressure. Likewise, the P_m and P_L for Moment load case are scaled to 863,646 in-lbs [1], corresponding to Service Level B conditions, which includes deadweight and OBE seismic loads [1].
3. The Q term in (P_L+P_B+Q) indicates the maximum thermal stress range between the four transients. The range is taken as the sum of the two largest Q values, for each stress path evaluated.

Table 5-4: Code Stress Evaluation for Service Level C/D Loads

Path	Material	P_m (ksi)	$1.2S_m$ (ksi)	P_L+P_B (ksi)	$1.8S_m$ (ksi)
Inside Path Location					
1	Alloy 182	12.61	27.96	15.41	41.94
2	Alloy 182	13.07	27.96	15.83	41.94
3	Alloy 182	13.57	27.96	16.66	41.94
4	SA-182, F304	11.46	19.92	10.58	29.88
5	SA-182, F304	16.37	19.92	20.00	29.88
11	Alloy 182	12.07	27.96	13.80	41.94
12	Alloy 182	12.44	27.96	13.85	41.94
13	Alloy 182	12.86	27.96	14.25	41.94
14	SA-182, F304	11.84	19.92	11.28	29.88
15	SA-182, F304	15.16	19.92	16.57	29.88
Outside Path Location					
1	Alloy 182/52M	12.61	27.96	9.81	41.94
2	Alloy 182/52M	13.07	27.96	10.33	41.94
3	Alloy 182/52M	13.57	27.96	10.54	41.94
4	SA-508 / Alloy 52M	11.46	19.92	13.28	29.88
5	SA-182, F304 / Alloy 52M	16.37	19.92	13.25	29.88
11	Alloy 182/52M	12.07	27.96	10.35	41.94
12	Alloy 182/52M	12.44	27.96	11.03	41.94
13	Alloy 182/52M	12.86	27.96	11.47	41.94
14	SA-508 / Alloy 52M	11.84	19.92	16.79	29.88
15	SA-182, F304 / Alloy 52M	15.16	19.92	14.23	29.88

Notes:

1. All units are in ksi.
2. The P_m and P_L for Pressure load case are conservatively scaled to 1,423 psi design pressure. Likewise, the P_m and P_L for Moment load case are scaled to 1,382,839 in-lbs [1], corresponding to Service Level C/D conditions, which includes deadweight and SSE seismic loads [1].

Table 5-5: Event Cycles

Thermal Transients	No. of Cycles
Startup / Shutdown	120
Design Pressure Test	130
Loss of Feedwater Heater	80
Scram	180
Single Relief or Safety Valve Blowdown	10
Loss of AC Power[1]	15
Seismic During Normal Operation	10

Notes:

1. Note that the Loss of A.C. Power transient has three internal stress reversals (cycles), and therefore the number of cycles considered for fatigue usage and crack growth calculations are multiplied by three in the evaluations.
2. Number of cycles specified for 40 year period.

Table 5-6: Materials for Fatigue Evaluation

Path (1)	**Surface**	**Material** (2)
1	Inside	Alloy 182
	Outside	Alloy 182/52M
2	Inside	Alloy 182
	Outside	Alloy 182/52M
3	Inside	Alloy 182
	Outside	Alloy 182/52M
4	Inside	SA-182, F304
	Outside	SA-508 / Alloy 52M
5	Inside	SA-182, F304
	Outside	SA-182, F304 / Alloy 52M
11	Inside	Alloy 182
	Outside	Alloy 182/52M
12	Inside	Alloy 182
	Outside	Alloy 182/52M
13	Inside	Alloy 182
	Outside	Alloy 182/52M
14	Inside	SA-182, F304
	Outside	SA-508 / Alloy 52M
15	Inside	SA-182, F304
	Outside	SA-182, F304 / Alloy 52M

Notes:

1. See Figure 5-1 for illustration of indicated locations.
2. Identified in Reference 14.

Table 5-7: Fatigue Usage Results

Path[2]	Material	P_L+P_B+Q+F (ksi)	Sa (ksi)	Allowable Cycles	Applied Cycles[1]	Fatigue Usage
Inside Location						
1	Alloy 182	69.06	34.53	2.55E+05	775	0.003
2	Alloy 182	65.88	32.94	3.42E+05	775	0.002
3	Alloy 182	82.46	41.23	9.44E+04	775	0.008
4	SA-182, F304	60.38	30.19	6.11E+05	775	0.001
5	SA-182, F304	52.50	26.25	1.00E+06	775	0.001
11	Alloy 182	67.83	33.91	2.85E+05	775	0.003
12	Alloy 182	64.37	32.18	3.96E+05	775	0.002
13	Alloy 182	80.02	40.01	1.11E+05	775	0.007
14	SA-182, F304	61.57	30.79	5.27E+05	775	0.001
15	SA-182, F304	48.76	24.38	1.00E+06	775	0.001
Outside Location						
1	Alloy 182/52	38.05	19.03	1.00E+06	775	0.001
2	Alloy 182/52	33.78	16.89	1.00E+06	775	0.001
3	Alloy 182/52	69.51	34.76	2.45E+05	775	0.003
4	SA-508 / Alloy 52M	76.37	38.18	1.00E+04	775	0.078
5	SA-182, F304 / Alloy 52M	74.11	37.06	1.68E+05	775	0.005
11	Alloy 182/52	38.89	19.45	1.00E+06	775	0.001
12	Alloy 182/52	34.86	17.43	1.00E+06	775	0.001
13	Alloy 182/52	70.28	35.14	2.29E+05	775	0.003
14	SA-508 / Alloy 52M	84.15	42.07	7.39E+03	775	0.105
15	SA-182, F304 / Alloy 52M	76.36	38.18	1.43E+05	775	0.005

Notes:
1. Note that the applied cycles = 120 + 130 + 180 + 345 (115 x 3 LOP) = 775 cycles (Section 5.5.1)
2. See Figure 5-1 for an illustration of indicated locations.

Table 5-8: Fatigue Usage Using Fatigue Reduction Factor

Path	Material	P_L+P_B+Q (ksi)	P_L+P_B+Q+F[1] (ksi)	Sa (ksi)	Allowable Cycles	Applied Cycles	Fatigue Usage
Inside Path Location							
1	Alloy 182	56.28	101.30	50.65	3.18E+04	775	0.024
2	Alloy 182	54.75	98.55	49.27	3.65E+04	775	0.021
3	Alloy 182	68.37	123.07	61.54	1.21E+04	775	0.064
4	SA-182, F304	40.42	72.76	36.38	1.86E+05	775	0.004
5	SA-182, F304	39.29	70.72	35.36	1.00E+06	775	0.001
11	Alloy 182	55.32	99.57	49.79	3.46E+04	775	0.022
12	Alloy 182	53.43	96.18	48.09	4.13E+04	775	0.019
13	Alloy 182	66.08	118.95	59.48	1.43E+04	775	0.054
14	SA-182, F304	40.71	73.27	36.64	1.79E+05	775	0.004
15	SA-182, F304	35.87	64.56	32.28	3.88E+05	775	0.002
Outside Path Location							
1	Alloy 182/52M	29.71	53.47	26.73	1.00E+06	775	0.001
2	Alloy 182/52M	27.34	49.21	24.60	1.00E+06	775	0.001
3	Alloy 182/52M	51.07	91.92	45.96	5.20E+04	775	0.015
4	SA-508 /Alloy 52M	49.63	89.34	44.67	6.19E+03	775	0.125
5	SA-182, F304 /Alloy 52M	40.68	73.23	36.62	1.80E+05	775	0.004
11	Alloy 182/52M	30.73	55.31	27.65	1.00E+06	775	0.001
12	Alloy 182/52M	28.53	51.36	25.68	1.00E+06	775	0.001
13	Alloy 182/52M	51.91	93.44	46.72	4.78E+04	775	0.016
14	SA-508 /Alloy 52M	53.18	95.72	47.86	5.04E+03	775	0.154
15	SA-182, F304 /Alloy 52M	41.99	75.58	37.79	1.51E+05	775	0.005

Note 1: P_L+P_B+Q+F is equal to P_L+P_B+Q multiplied by a reduction factor of 1.8

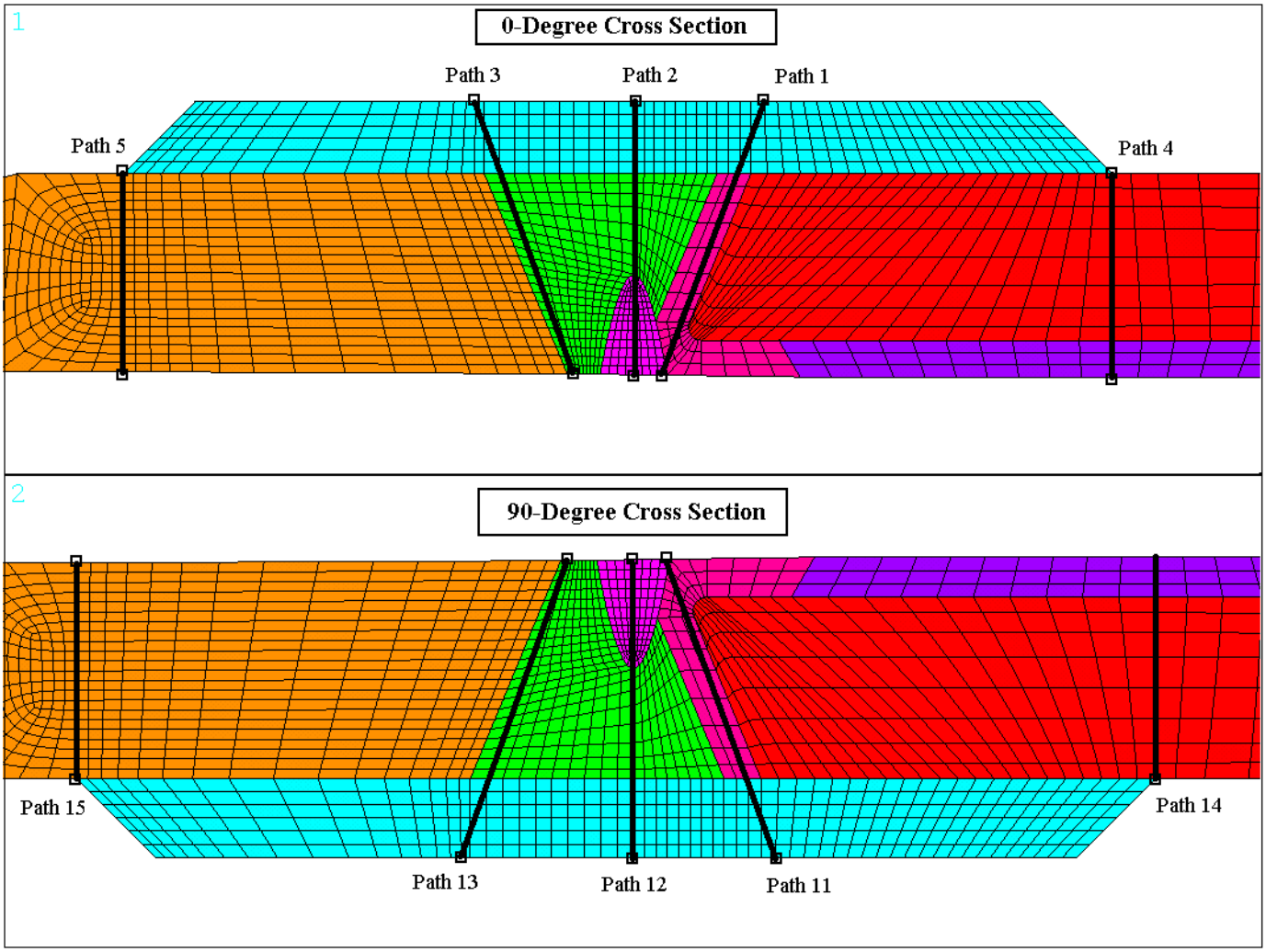

Figure 5-1: Sections Used for Section III Evaluation

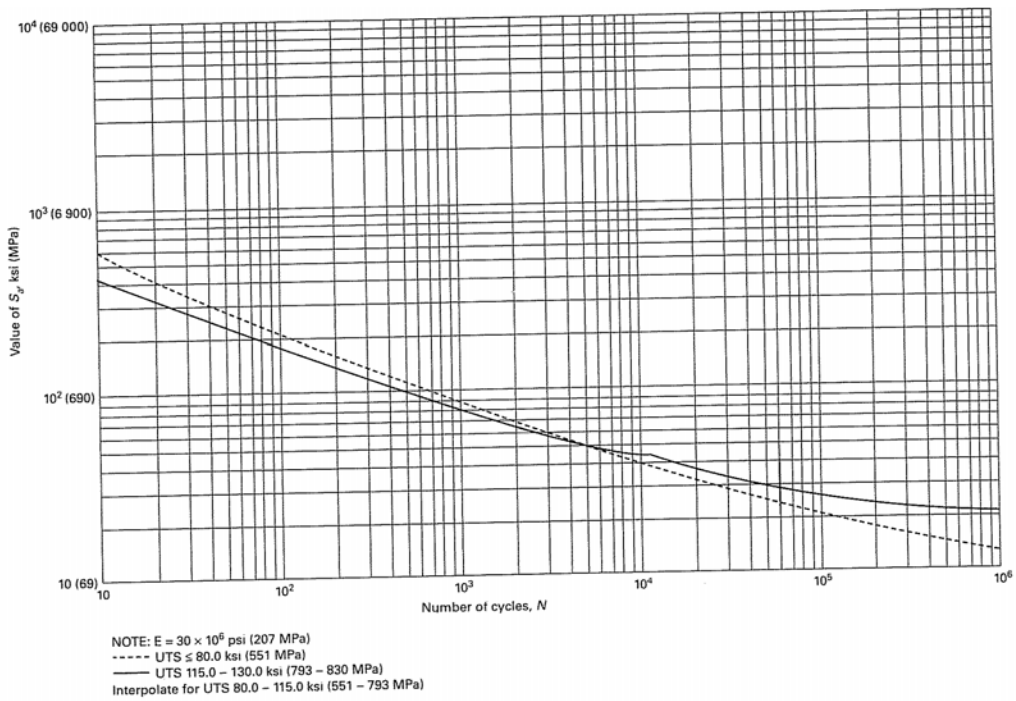

(a) Low Alloy Steel

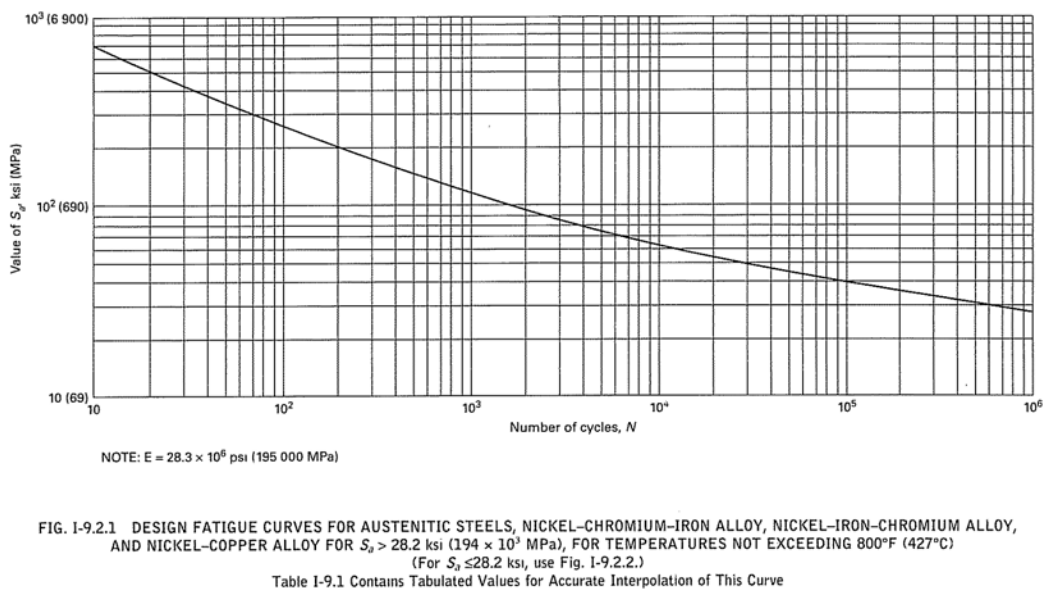

(b) Ni-Cr-Fn / Austenitic Steel

Figure 5-2: Material Fatigue Curves

6.0 CRACK GROWTH EVALUATION

6.1 Background

In this section, crack growth in the DMW section is considered for both IGSCC and fatigue mechanisms. ISI-ALT-08-02 requires that potential flaw growth due to fatigue and the mechanism believed to have caused the flaw (IGSCC) be considered. The weld metal to be used for the overlay repair is Alloy 52M, which is very resistant to IGSCC.

6.2 Technical Approach

The technical approach used in this evaluation is to consider the through-wall stress intensity factor (K) distribution associated with the postulated DMW flaw, using the post-weld overlay stresses at operating conditions. If the K distribution is such that it is negative at the crack tip, then no IGSCC growth will be expected. If the K is positive, then a flaw growth evaluation will be performed to determine the adequacy of the weld overlay repair. From a fatigue standpoint, the ΔK distribution for the pertinent thermal cycles is used.

6.3 Fatigue Crack Growth

The fatigue crack growth evaluation was performed in Reference 14. The crack models shown in Figure 6-1 are taken from the library of the fracture mechanics program pc-CRACK [16] for the fracture mechanics and crack growth analysis. A crack model of a full circumferential crack in a cylinder with t/R = 0.2 (Figure 6-1 [16]) is used with the axial stresses, and a model of an infinitely long longitudinal crack in a cylinder (with t/R = 0.2) is used with the hoop stresses.

The fatigue crack growth law for Alloy 690 (which bounds that of the Alloy 600 DMW base metal) is obtained from Reference 18:

$$\frac{da}{dN} = C_{A690}(1-0.82R)^{-2.2}\Delta K^{4.1} \qquad (1)$$

$$C_{A690} = 5.423x10^{-14} + 1.83x10^{-16}T - 1.725x10^{-1.8}T^2 + 5.49x10^{-21}T^3 \qquad (2)$$

where T is in °C and ΔK is in MPa-√m.

Using an operating temperature of 546 °F, assuming a R ratio of 0.9, and converting the unit of ΔK from MPa-√m to Ksi-√in, the fatigue crack growth law (in in/cycle) in Equation (1) becomes

$$\frac{da}{dN} = 6.8617x10^{-12}\Delta K^{4.1} \qquad (3)$$

The fatigue cycles shown in Table 5-5 are grouped as follows (note that, since these transient events are not defined in the design report [10] for the recirculation inlet nozzle, the Blowdown transient and Loss of Feedwater transient have been grouped with the Loss of A.C. Power transient, which has the highest stress results):

Startup/Shutdown:	120 cycles
Design Pressure Test:	130 cycles
Scram:	180 cycles
LOP:	115 x (3 internal cycles) = 345 cycles (includes 15 LOP cycles, 10 blowdown, 10 seismic, and 80 Loss of Feedwater cycles)

These fatigue cycles are distributed evenly over 40 years. For conservatism, the thermal and pressure ranges are assumed as the full fluctuation from zero to maximum stress. The full piping moment (863,646 in-lbs [1]) is conservatively added to the maximum K value for all cycles. An initial crack depth of 0.260" (as reported in the examination summary sheet [9]) is used in the fatigue crack growth calculation. Fatigue crack growth threshold is assumed to be zero.

For the crack growth evaluation, through-wall stress profiles were extracted for the selected paths for the load cases of unit 1,000 psi pressure, unit 1,000 in-lb piping moment, weld residual stress, and thermal transients. For the thermal transients, the through-wall stress profiles were obtained at the times of maximum linearized membrane-plus-bending stress. The through-wall stress profiles at the DMW are presented in Figure 6-2 through Figure 6-8. The residual through-wall stress profiles (for both room temperature and normal operating conditions) at the DMW are presented in Figure 6-9. The curve-fit results of these through-wall stress profiles are presented in Tables 6-1 to 6-7.

For fracture mechanics and crack growth calculation, various paths were selected for evaluation based on the indication location. The stress intensity factor results are presented in Figure 6-10 for the circumferential flaw, and Figure 6-12 for the axial flaw. The total applied normal operating

condition (NOC) IGSCC stress intensity factor is also presented in Figures 6-10 and 6-12, for the circumferential and axial flaws, respectively. The NOC stress intensity factor is the combination due to normal operating stresses (at 546°F and 1,000 psi) including residual stresses and piping moments (deadweight plus seismic loading). It is shown that, for the circumferential flaw, the applied stress intensity factor during the normal steady state operation is tensile then compressive along the thickness at the DMW section, and therefore IGSCC will be active in the tensile regions.

The fatigue crack growth results are presented in Figure 6-11 for the circumferential flaw, and Figure 6-13 for the axial flaw. The circumferential flaw (with initial flaw depth of 0.260 inches) grows to 0.744 inches in 40 years (see Table 6-9). The axial flaw grows from 0.260 inches to 0.270 inches.

6.4 IGSCC Flaw Growth

ISI-ALT-08-02 requires that potential flaw growth due to the mechanism believed to have caused the flaw (IGSCC) be considered. In addition to fatigue crack growth, IGSCC must be considered since the steady-state normal operating stress intensity factors are shown to be tensile for some flaw depths in the case of a postulated circumferential flaw, as shown in Figure 6-10. The IGSCC growth rates (for hydrogen water chemistry) are obtained from Reference 19 as follows:

$$\frac{da}{dt} = C_o K_I^{\,n} \quad \text{in/hr for } K_I \leq 25 \text{ ksi}\sqrt{\text{in}} \qquad (4)$$

$$\frac{da}{dt} = C_1 \quad \text{in/hr for } K_I > 25 \text{ ksi}\sqrt{\text{in}} \qquad (5)$$

where,

K_I = stress intensity factor at flaw tip (ksi√in)
C_o = 3.2×10^{-10}
C_1 = 5.0×10^{-6}
n = 3.0

Although a 10-year inspection interval is assumed; 40 years of IGSCC growth is evaluated. The stress intensity factor and fatigue crack growth calculation are performed using **pc-CRACK** [16].

Sustained steady-state normal operating stresses are the only stresses that need to be considered for the SCC growth analysis. The sustained stress intensity factors due to stress (residual, normal operating temperature and pressure) and full piping loads, conservatively including deadweight and seismic loading (moment of 863,646 in-lbs [1]), are used in the SCC growth analysis. Using the maximum NOC K of 16.3 ksi-in$^{1/2}$ for the circumferential flaw (Figure 6-10, at approximately 0.24" crack depth) yields approximately 0.484" of growth during the 40 year interval, as reported in Table 6-9. The NOC hoop stresses and stress intensity factors for the axial flaw are compressive (see Figure 6-12), and therefore no IGSCC growth occurs for the axial flaw, as shown in Table 6-9.

The fracture toughness of Alloy 690 weld metal is presented in Table 6-8, as obtained from Reference 21. It is shown that the fracture toughness for Alloy 82/52 is very high at high temperature and water environment. Conservatively using the equivalent linear elastic fracture toughness for this evaluation, the minimum fracture toughness of 239 ksi-√in is higher than any total applied stress intensity factor shown in Figure 6-10 and Figure 6-12, and satisfies the maximum linear elastic fracture mechanics safety factor of √10 [2].

Thus, the weld overlay mitigates the weld against stress corrosion cracking. Hence, from an IGSCC viewpoint, the overlay repair for the DMW weld is considered a long-term fix, subject to NRC mandated inspections in Generic Letter 88-01 [4], as modified by BWRVIP-75 [17].

6.5 Extended Power Uprate (EPU) Considerations

Note that the transient conditions evaluated in Reference 12 do not include extended power uprate (EPU) conditions. Rather, the thermal, pressure, and mechanical loadings, used to determine the stress and fatigue results reported herein, were based on original plant design conditions. Therefore, the results were factored to account for EPU. The EPU task report [20] documents an increase in pressure from 1,000 psig to 1,048 psig, which is an increase of 4.8%. The report also documents increases in temperature for the reactor vessel Regions A, B, and C. Of the revised temperatures shown, the largest increase is from 435°F to 441°F, which is an increase of approximately 1.6% in Region B where the recirculation nozzle is located. Since the detailed crack growth calculations [14] were performed using the design pressure of 1,423 psi (rather than the operating pressure), no additional factors were added to the pressure stress results. The crack growth results were increased by 1.6% to account for increases in thermal stress. The amount of fatigue crack growth was seen to be negligible (as shown in Table 6-9), and therefore the increase in fatigue crack growth due to EPU is negligible.

The increase in stress corrosion cracking due to an increase in thermal stresses is a non-linear relationship. Therefore, the thermal stresses (and piping moments loads) were increased by 1.6%, and the 'K vs a' solution obtained from pc-CRACK [16] for the circumferential flaw model. The resulting maximum IGSCC K value increased from 16.3 ksi to 16.9 ksi [14]. The maximum K of 16.9 ksi was then input to Equation (4) in Section 6.4, resulting in 0.541" of growth, compared to 0.484" reported in Table 6-9. Therefore, the crack depth at 40 years will be approximately 0.260" + 0.541" = 0.801", which is approximately 67% of the base metal thickness in the DMW flaw region.

Table 6-1: Curve-fit Coefficients, Unit Pressure

Stress Comp	Path	Curvefit Coefficient (psi)			
		C_0	C_1	C_2	C_3
Axial	1	1189.2	-821.0	566.9	-136.5
	2	1295.2	-757.2	417.3	-121.3
	3	1523.7	-807.1	359.3	-157.8
	11	2503.1	-782.0	841.7	-219.0
	12	2519.0	-617.9	490.5	-126.6
	13	2650.0	-697.4	400.5	-183.6
Hoop	1	4775.6	-2314.7	1262.2	-337.8
	2	4855.2	-1792.9	460.5	-101.6
	3	5063.5	-1771.3	381.0	-114.2
	11	3364.8	-662.2	705.6	-246.3
	12	3305.6	-219.6	173.0	-56.2
	13	3259.5	-239.7	297.6	-97.4

Table 6-2: Curve-fit Coefficients, Unit Moment

Stress Comp	Path	Curvefit Coefficient (psi)			
		C_0	C_1	C_2	C_3
Axial	1	5.1901	-1.8538	1.1005	-0.3491
	2	5.1020	-1.3783	0.4032	-0.0615
	3	5.1483	-1.2002	0.2684	-0.0961
	11	5.1934	-1.8579	1.1018	-0.3501
	12	5.1055	-1.3834	0.4036	-0.0618
	13	5.1510	-1.2035	0.2678	-0.0959
Hoop	1	-0.4813	-0.4219	0.1480	-0.0242
	2	-0.5820	-0.6632	0.2537	-0.0437
	3	-0.7380	-0.7779	0.2939	-0.0768
	11	-0.5082	-0.3859	0.1383	-0.0213
	12	-0.6077	-0.6281	0.2462	-0.0425
	13	-0.7621	-0.7440	0.2837	-0.0750

Table 6-3: Curve-fit Coefficients, Startup Transient

Stress Comp	Path	Curvefit Coefficient (psi)			
		C_0	C_1	C_2	C_3
Axial	1	-6812.9	28363.8	-22972.8	3998.4
	2	-740.9	3202.5	-2390.7	256.6
	3	-1264.8	4908.9	-4511.2	1231.4
	11	-6810.8	28370.5	-22970.3	3997.5
	12	-746.3	3198.5	-2390.6	256.6
	13	-1269.6	4905.1	-4510.3	1231.4
Hoop	1	6979.1	15075.2	-18351.4	3733.4
	2	7259.6	14223.9	-13468.0	1259.0
	3	6912.1	38078.8	-39997.9	10544.5
	11	7183.2	14727.2	-18244.9	3719.1
	12	7479.6	13882.8	-13369.2	1247.5
	13	7154.9	37781.3	-39937.0	10540.9

Table 6-4: Curve-fit Coefficients, Shutdown Transient

Stress Comp	Path	Curvefit Coefficient (psi)			
		C_0	C_1	C_2	C_3
Axial	1	8718.4	-14842.9	11511.1	-5340.0
	2	8843.6	-19547.9	16797.2	-6718.9
	3	5371.2	-7880.8	-736.6	2453.6
	11	8621.5	-14879.4	11479.4	-5329.7
	12	8754.4	-19600.5	16794.8	-6717.9
	13	5289.1	-7930.5	-727.3	2454.1
Hoop	1	22204.8	-37491.3	24407.9	-7573.0
	2	20075.7	-26187.2	10691.2	-2980.0
	3	20546.4	-13491.6	-3502.1	2057.4
	11	22607.0	-38004.2	24542.2	-7599.2
	12	20450.1	-26652.1	10786.4	-2995.2
	13	23924.6	-28959.7	14545.3	-3761.0

Table 6-5: Curve-fit Coefficients, Scram Transient

Stress Comp	Path	Curvefit Coefficient (psi)			
		C_0	C_1	C_2	C_3
Axial	1	-8106.1	34703.9	-28424.6	4986.8
	2	-7988.5	31282.7	-24560.0	4074.5
	3	-14494.6	52919.9	-51532.7	16124.8
	11	-8182.5	34663.4	-28452.9	4996.3
	12	-8061.3	31217.3	-24559.5	4075.2
	13	-14561.1	52857.1	-51518.5	16124.4
Hoop	1	7890.7	11461.9	-14651.2	2459.0
	2	8044.3	12239.2	-12582.6	984.0
	3	7684.8	34235.1	-37017.0	9612.6
	11	8181.3	11094.7	-14557.0	2440.6
	12	8339.1	11872.3	-12509.3	972.6
	13	7979.3	33898.8	-36959.4	9604.1

Table 6-6: Curve-fit Coefficients, Loss of A.C. Power (LOP) Transient

Stress Comp	Path	Curvefit Coefficient (psi)			
		C_0	C_1	C_2	C_3
Axial	1	6968.6	-2717.2	-2280.3	-1481.7
	2	6768.0	-5279.1	-1848.7	-286.1
	3	2025.4	9633.8	-23666.4	11154.9
	11	6886.2	-2742.5	-2310.7	-1471.2
	12	6692.3	-5319.3	-1851.8	-284.5
	13	1956.4	9594.6	-23658.1	11155.2
Hoop	1	26662.8	-35191.1	15608.1	-4519.3
	2	28108.3	-39226.9	18049.0	-4748.5
	3	28787.2	-21667.6	-2136.8	2419.2
	11	27048.8	-35693.0	15739.2	-4545.3
	12	28499.1	-39730.0	18157.2	-4766.1
	13	29186.7	-22141.2	-2045.7	2404.9

Table 6-7: Curve-fit Coefficients, Normal Operating Conditions

Stress Comp	Path	Curvefit Coefficient (psi)			
		C_0	C_1	C_2	C_3
Axial		**Residual at 70°F**			
	1	20561.6	-88824.4	6584.0	35919.5
	2	15317.7	-43737.4	-77990.4	80426.9
	3	43480.7	-152086.7	46426.3	29662.7
		Residual @ Normal Operating (546°F/1000 psi)			
	1	9338.9	-35088.7	-33385.5	40857.6
	2	5542.4	-2535.1	-98913.6	77227.1
	3	21295.9	-64774.9	-30565.3	50124.1
Hoop		**Residual at 70°F**			
	1	-65798.1	-148443.7	282795.3	-81928.6
	2	-62998.0	-273395.1	484836.9	-157697.1
	3	-29559.5	-271321.7	393983.3	-113402.3
		Residual @ Normal Operating (546°F/1000 psi)			
	1	-49849.1	-123642.6	245009.1	-72889.7
	2	-46040.8	-241572.6	437456.0	-145689.3
	3	-16847.8	-210885.4	322260.9	-94007.9

Table 6-8: Ni-Cr-Fe Fracture Toughness

Material	Orientation	Conditions	Jc (kJ/m^2)	Jc ($in\text{-}lb/in^2$)	K (ksi-√in)
EN82H	Longitudinal	338 °C/Air	803	4585	371
EN82H	Longitudinal	338 °C/Water	603	3443	321
EN82H	Transverse	338 °C/Air	332	1896	239
EN82H	Transverse	338 °C/Water	500	2855	293
EN52	Longitudinal	338 °C/Air	800	4568	370
EN52	Longitudinal	338 °C/Water	825	4710	376
EN52	Transverse	338 °C/Water	750	4282	358

Note: Values are obtained from $Jc = K^2/E$ [21]

Table 6-9: Crack Growth Summary

Flaw Type	Initial Crack Depth (1) (inch)	Crack Growth due to IGSCC (inch)	Crack Growth due to FCG, from **pc-CRACK** (inch)	Final Crack Depth (inch)	Final Depth, as a Percent of Base Metal Thickness (3)	Time (years)
Axial Flaw	0.260	0	0.010	0.270	23%	40
Circ. Flaw	0.260	0.484 (2)	0.0001	0.744	62%	40
Circ. Flaw (Including EPU)	0.260	0.530	0.0001	0.790	66%	40

Notes:
(1) The initial crack depth is set to 0.260", as reported in the examination summary sheet [9].
(2) Crack growth due to 40 years of IGSCC, using the maximum steady-state residual NOC K value of 16.3 ksi-in$^{1/2}$ (Figure 6-10, at approximately 0.24" crack depth).
(3) The original base metal thickness is approximately 1.2".

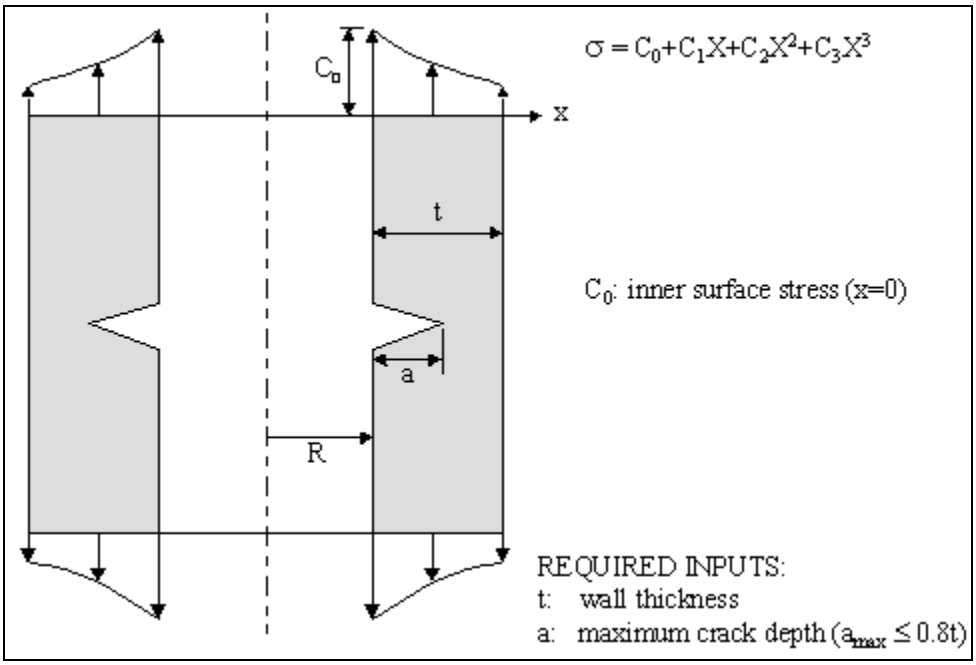

a) Full circumferential crack in a cylinder

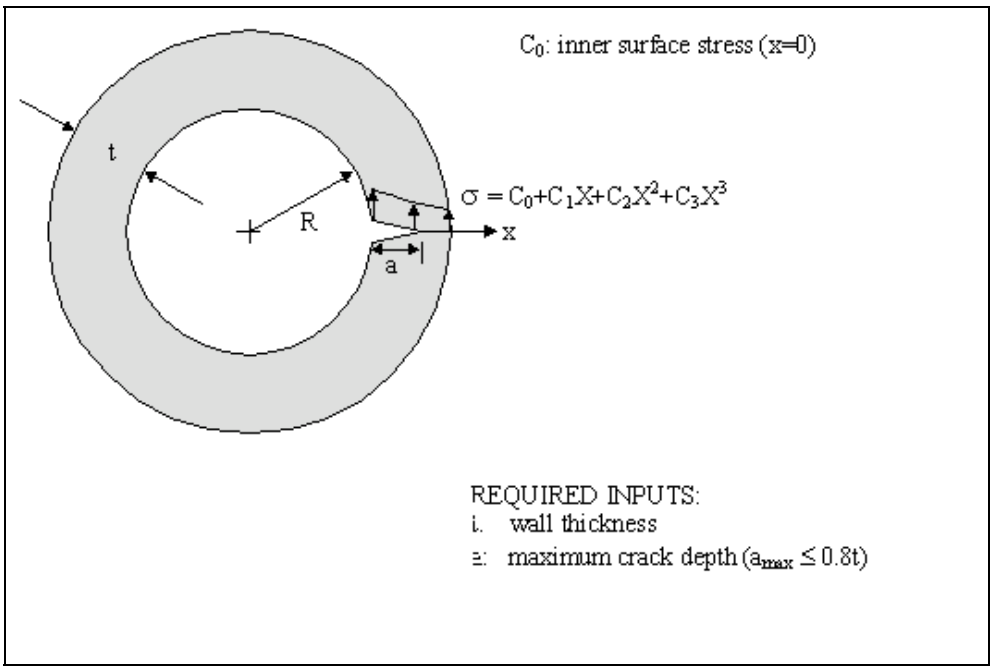

b) Axial crack in a cylinder

Figure 6-1: PC-Crack Flaw Models Used in Evaluation

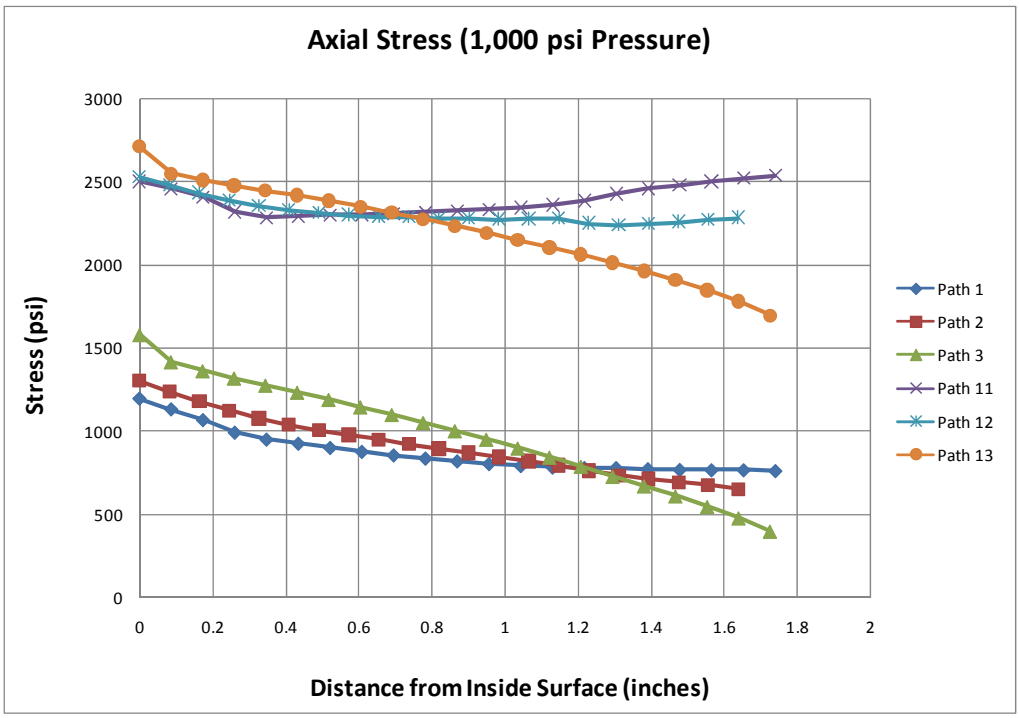

(a) Axial Stress

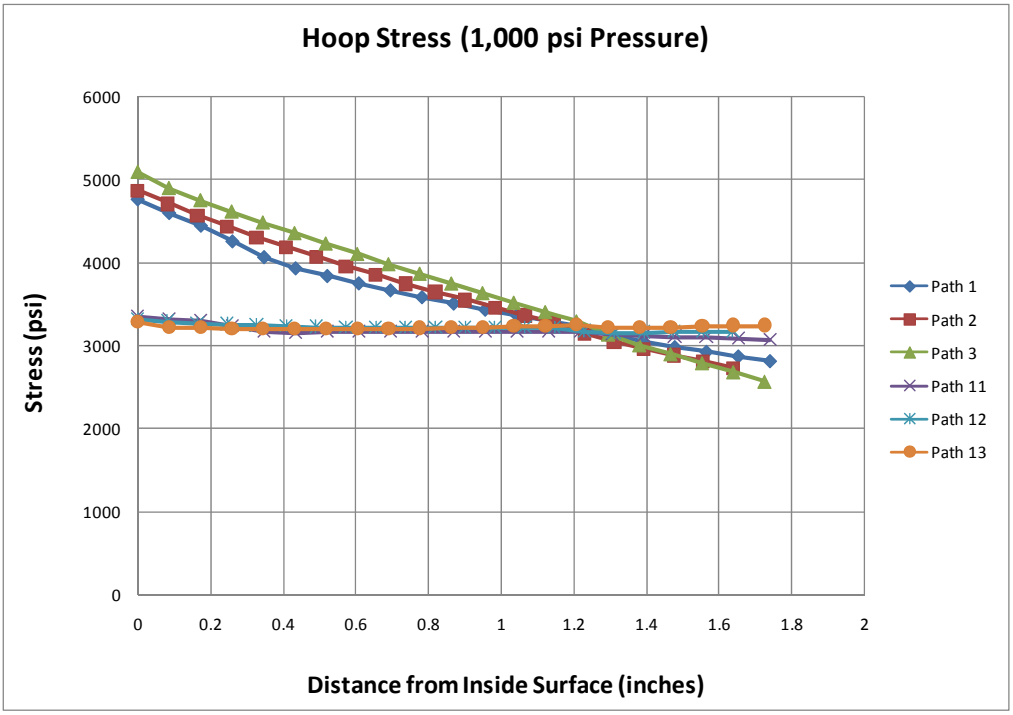

(b) Hoop Stress

Figure 6-2: Through-wall Stress Distribution, Unit Pressure

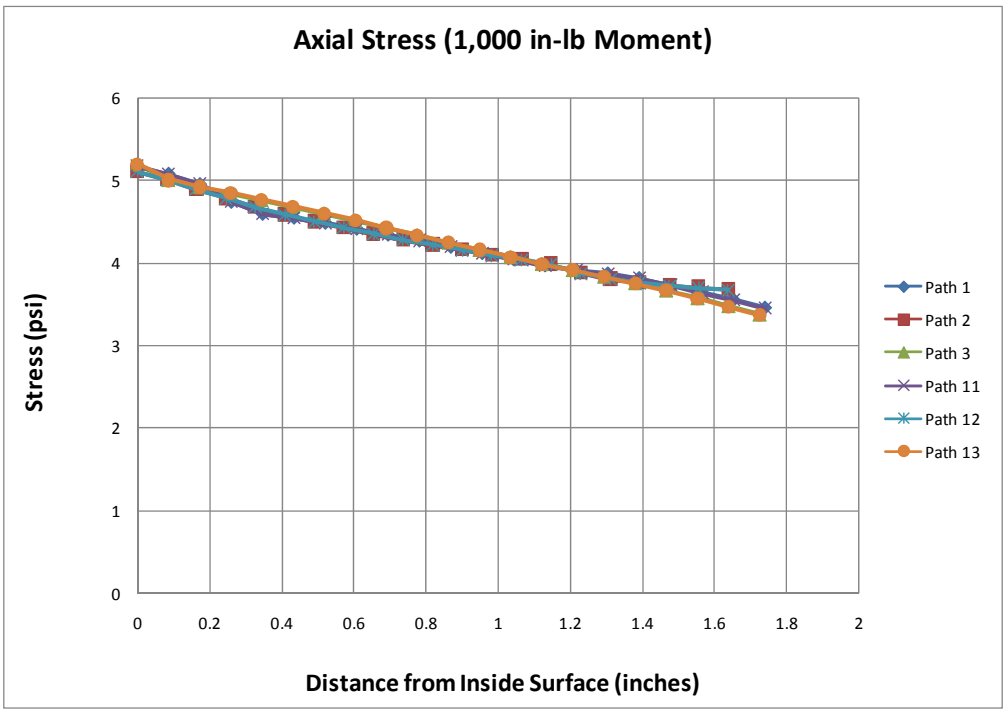

(a) Axial Stress

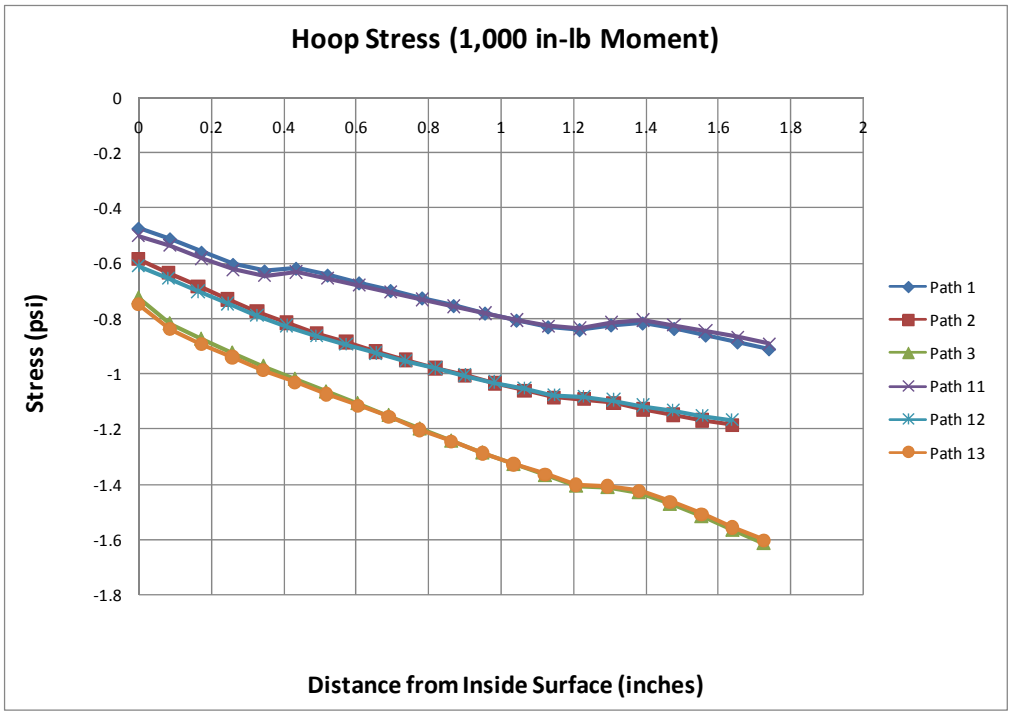

(b) Hoop Stress

Figure 6-3: Through-wall Stress Distribution, Unit Moment

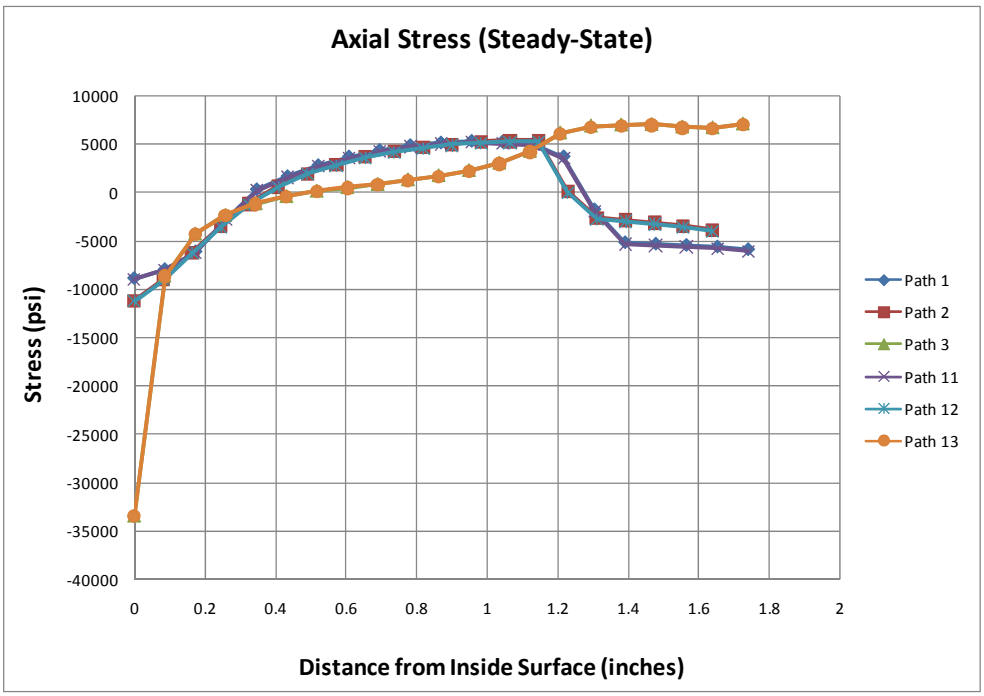

(a) Axial Stress

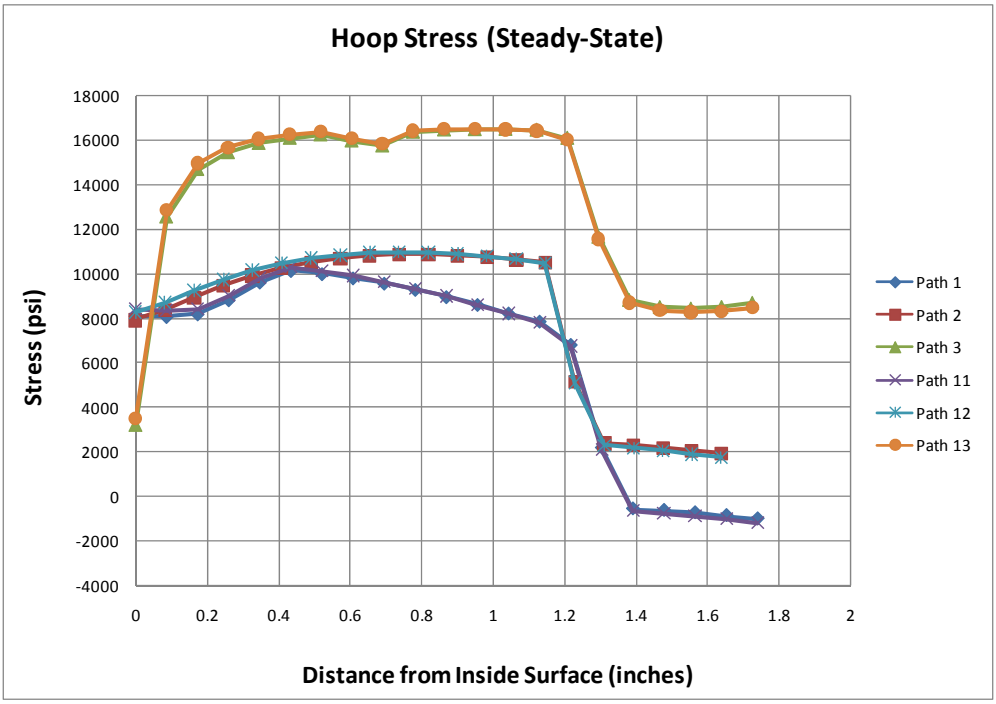

(b) Hoop Stress

Figure 6-4: Through-wall Stress Distribution, Steady-State

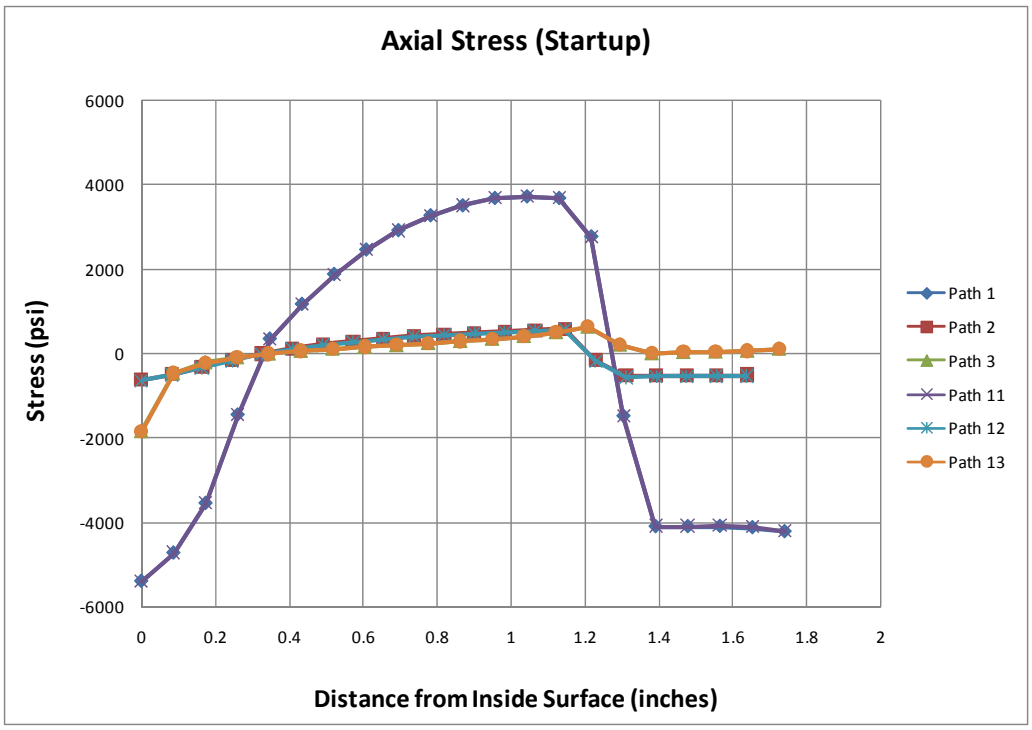

(a) Axial Stress

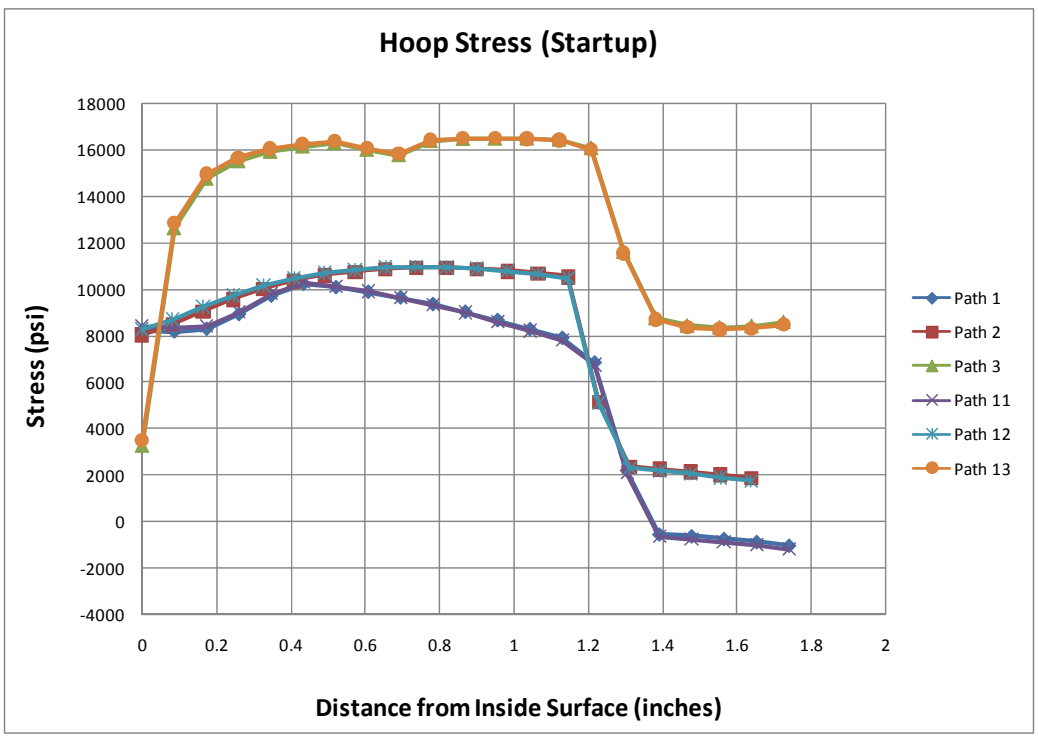

(b) Hoop Stress

Figure 6-5: Through-wall Stress Distribution, Startup Transient

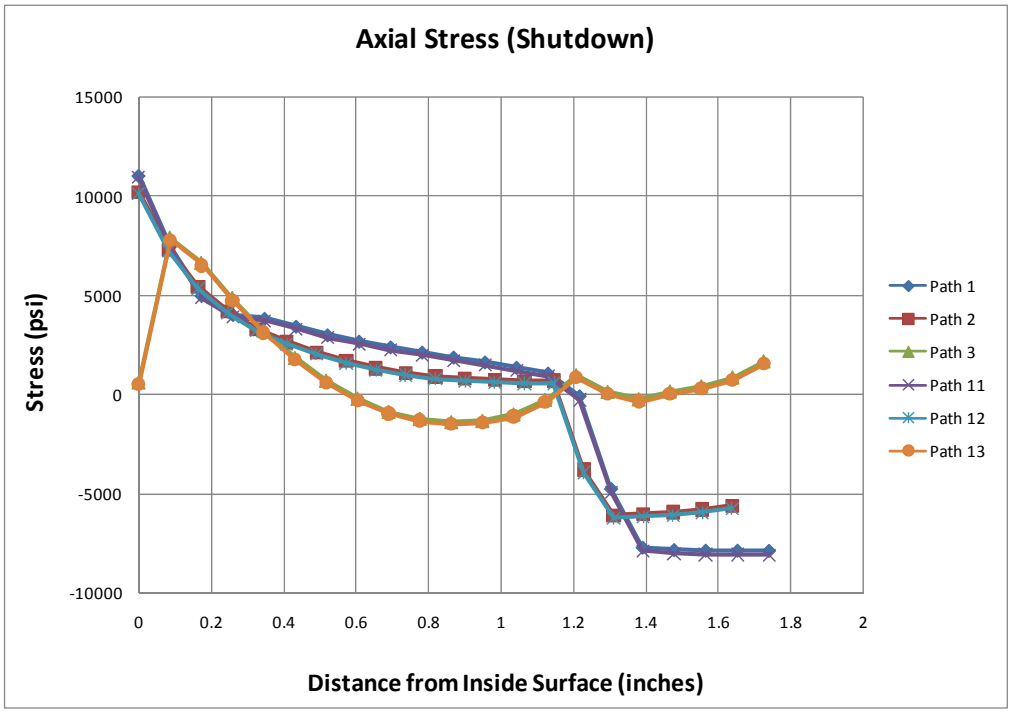

(a) Axial Stress

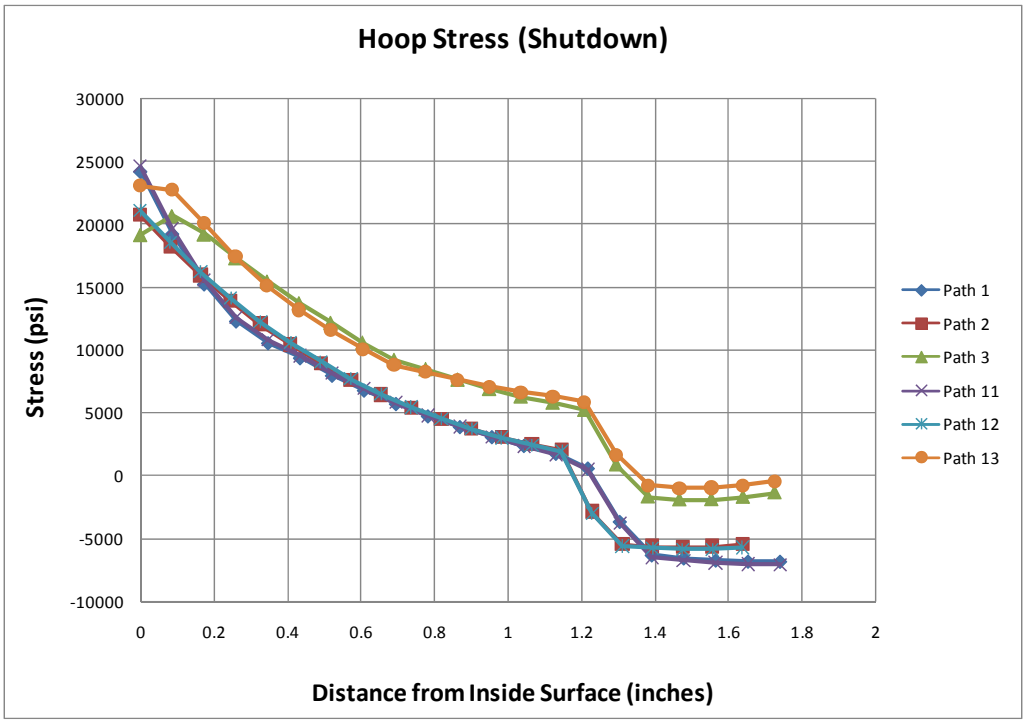

(b) Hoop Stress

Figure 6-6: Through-wall Stress Distribution, Shutdown Transient

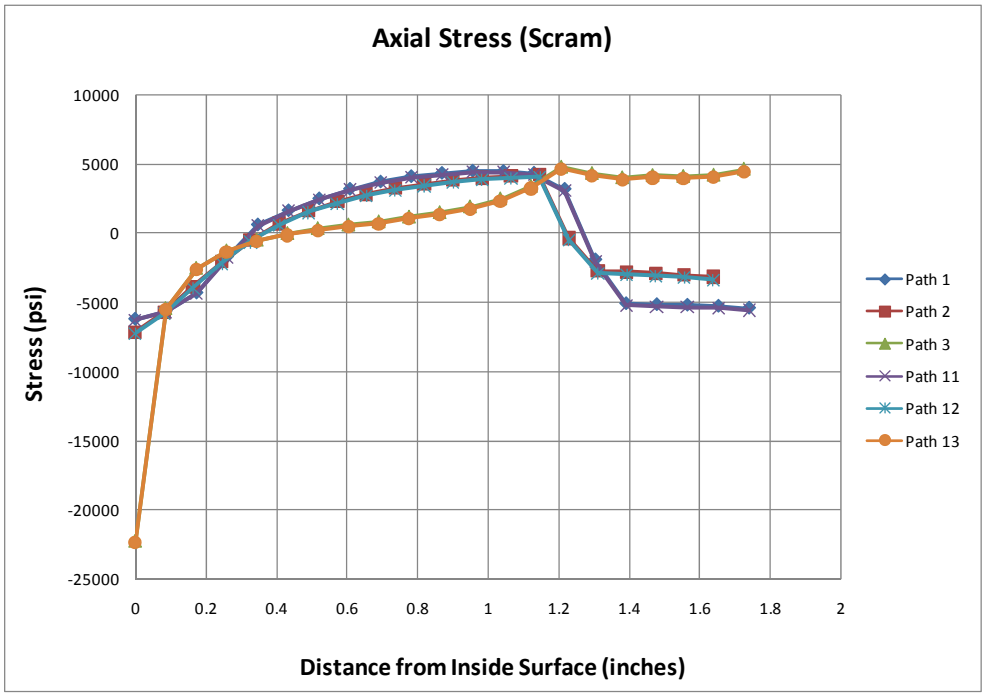

(a) Axial Stress

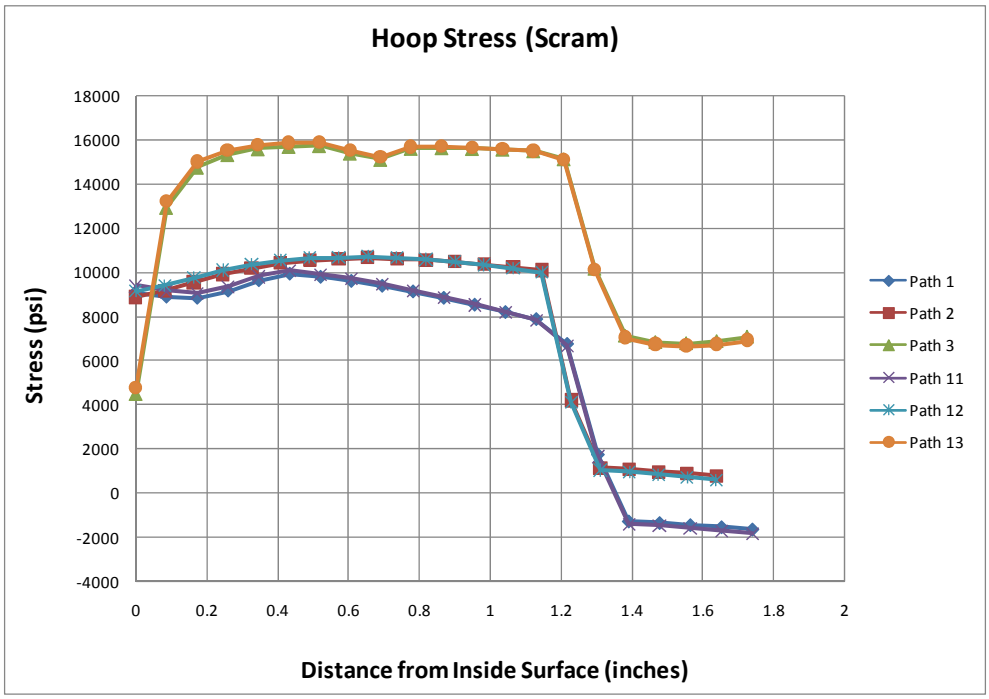

(b) Hoop Stress

Figure 6-7: Through-wall Stress Distribution, Scram Transient

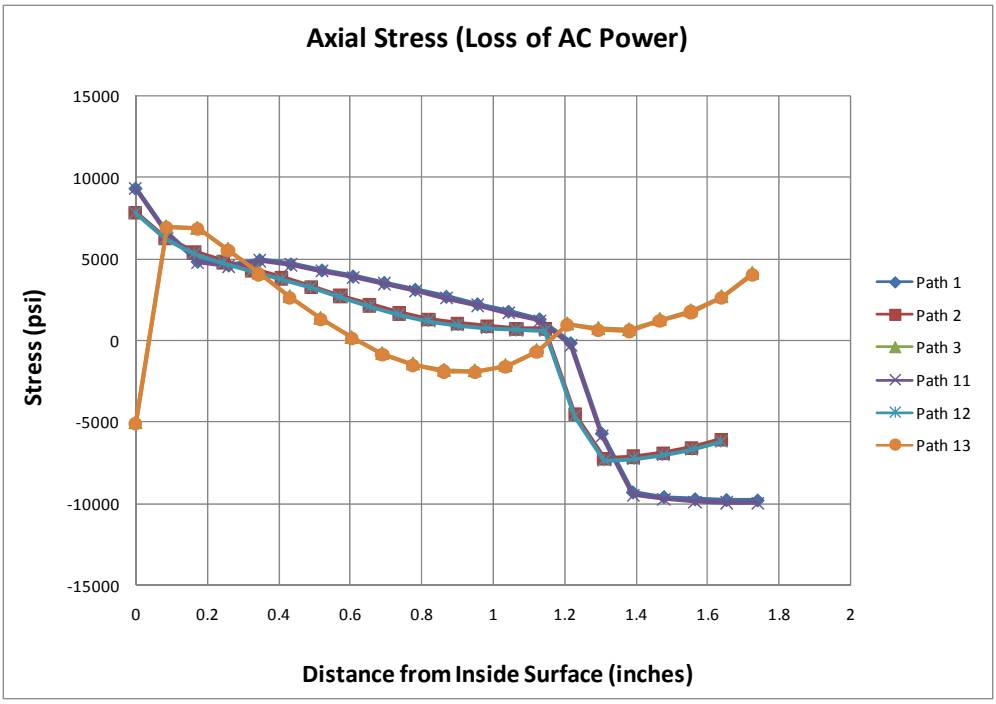

(a) Axial Stress

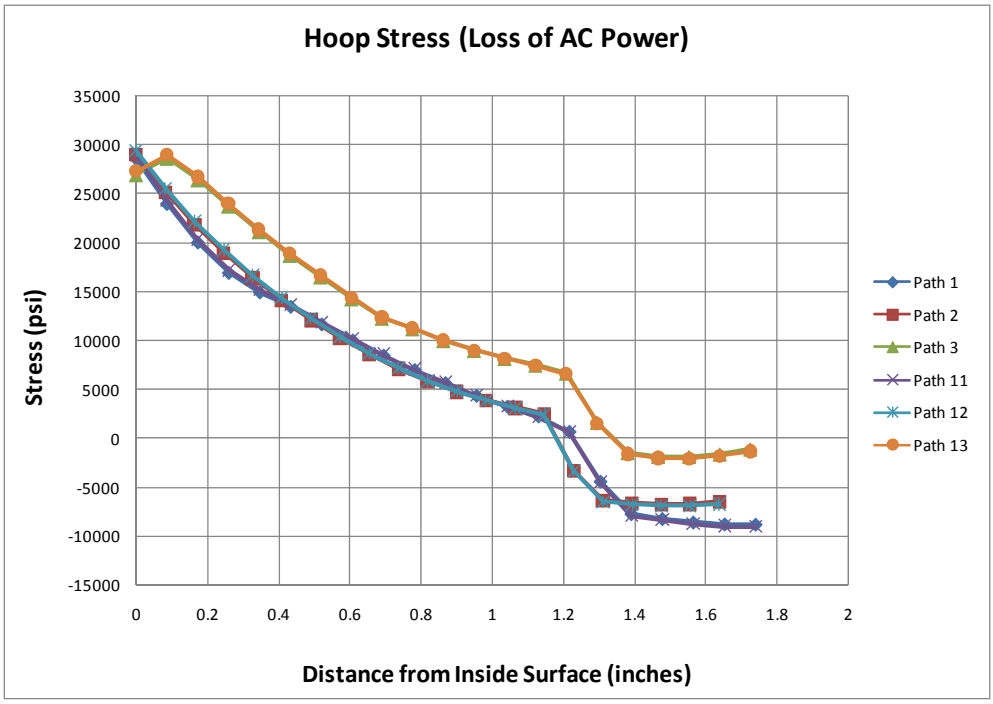

(b) Hoop Stress

Figure 6-8: Through-wall Stress Distribution, Loss of A.C. Power Transient

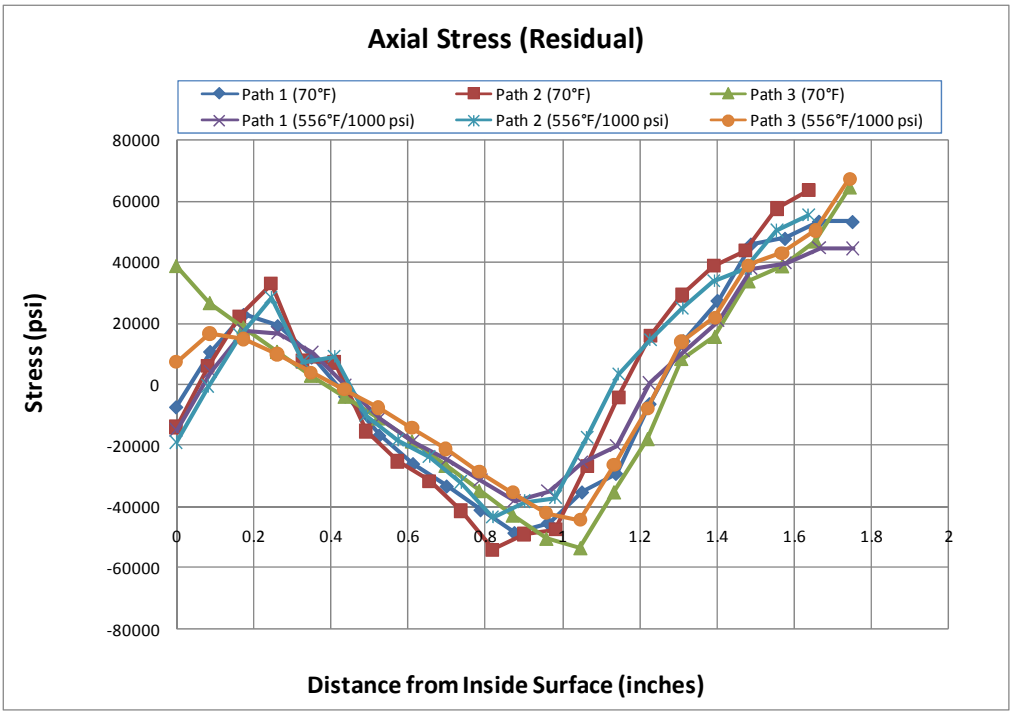

(a) Axial Stress

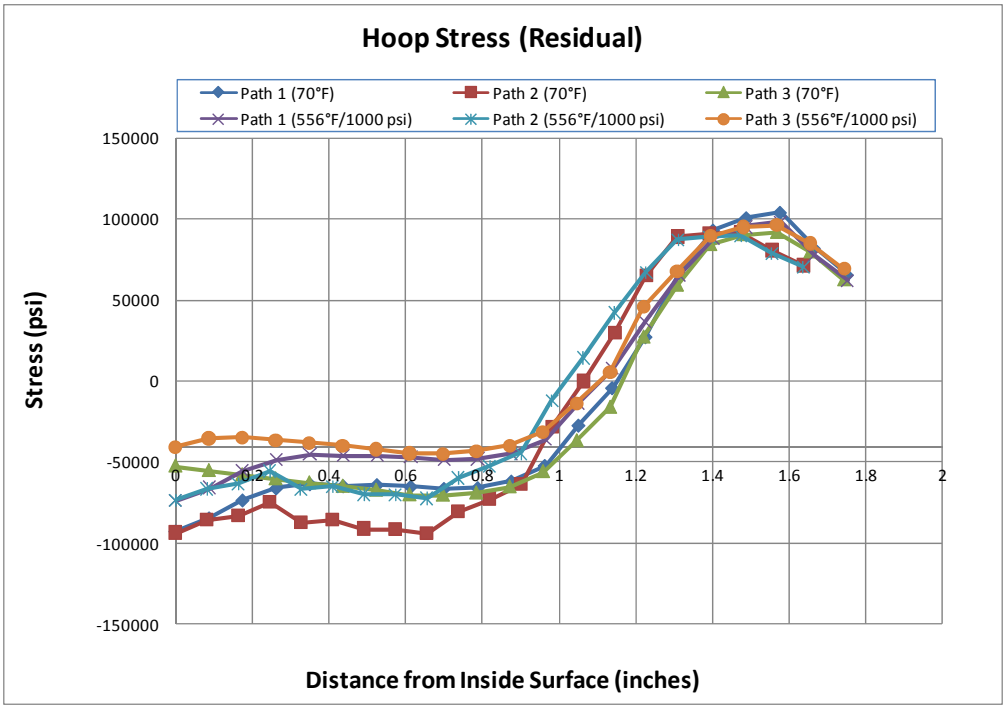

(b) Hoop Stress

Figure 6-9: Through-wall Stress Distribution, Residual

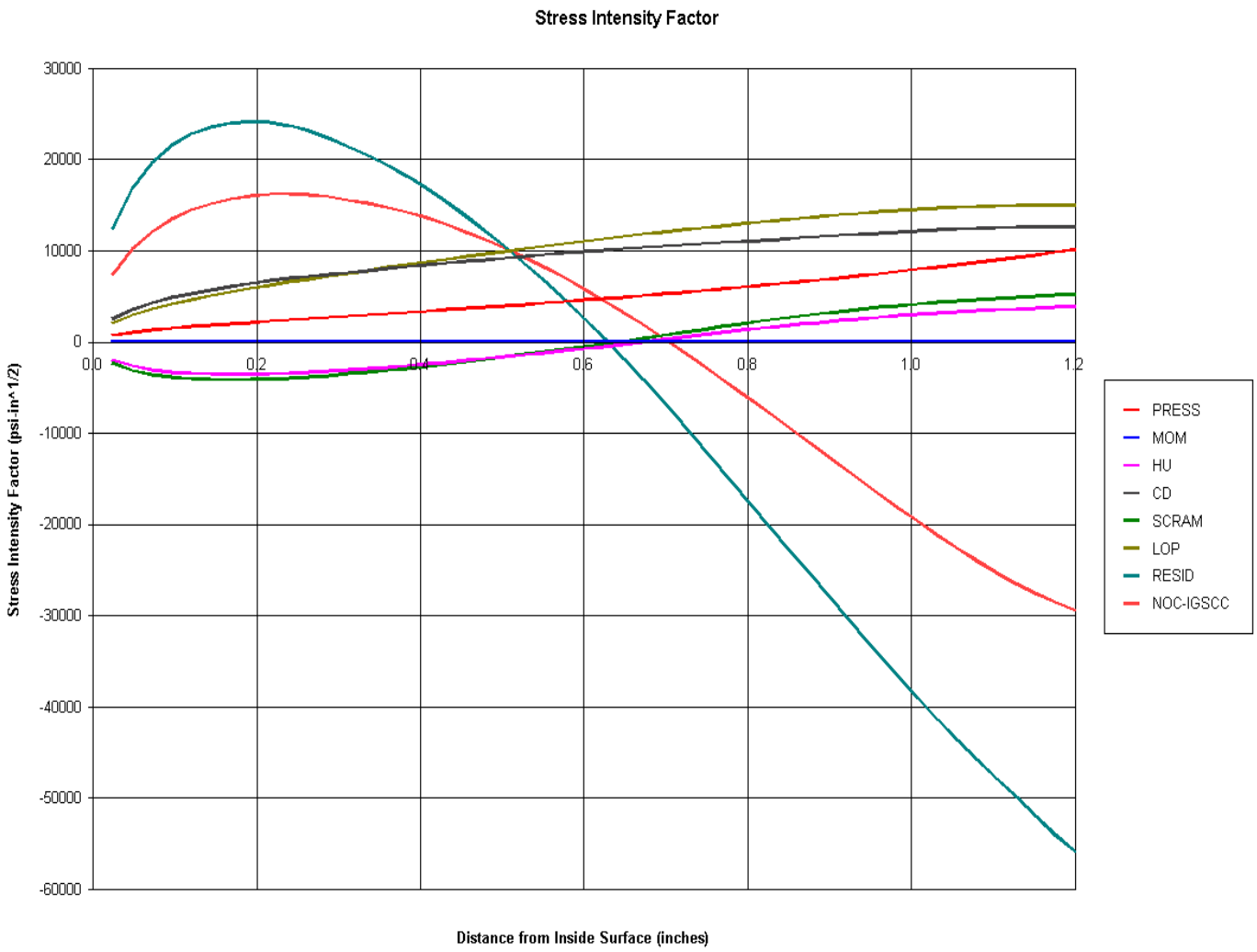

Figure 6-10: Stress Intensity Factors (Circumferential Flaw)

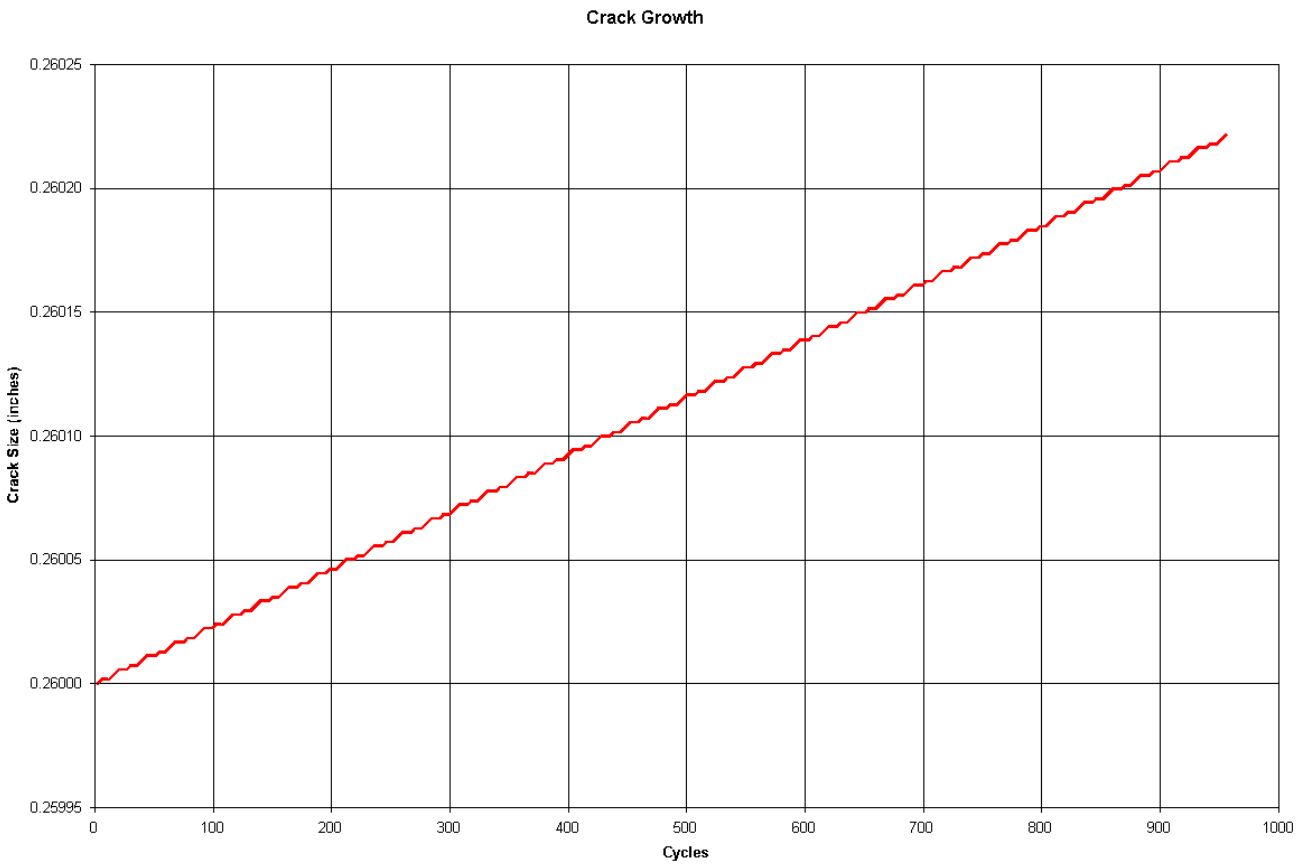

Figure 6-11: Fatigue Crack Growth Results (Circumferential Flaw)

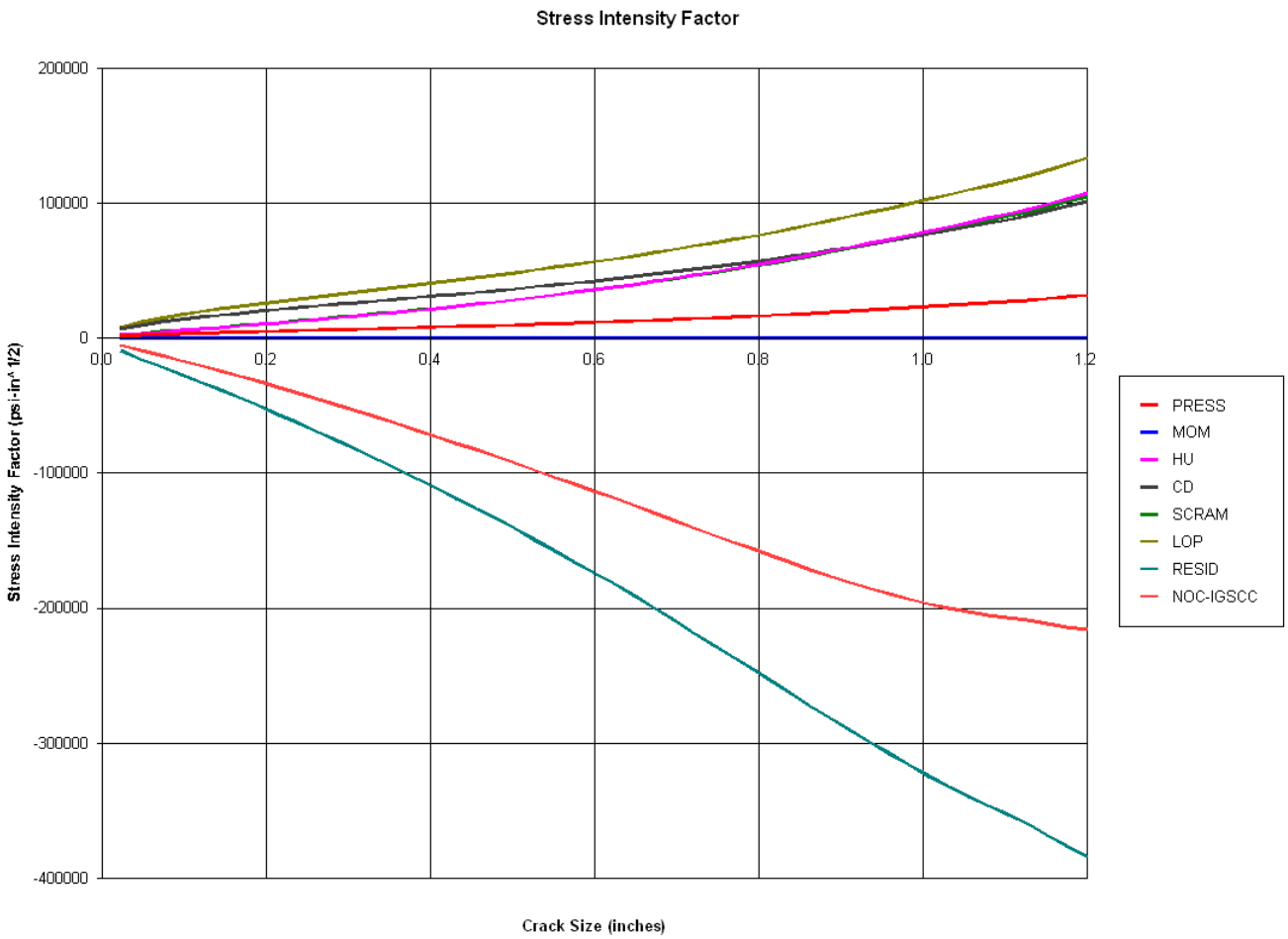

Figure 6-12: Stress Intensity Factors (Axial Flaw)

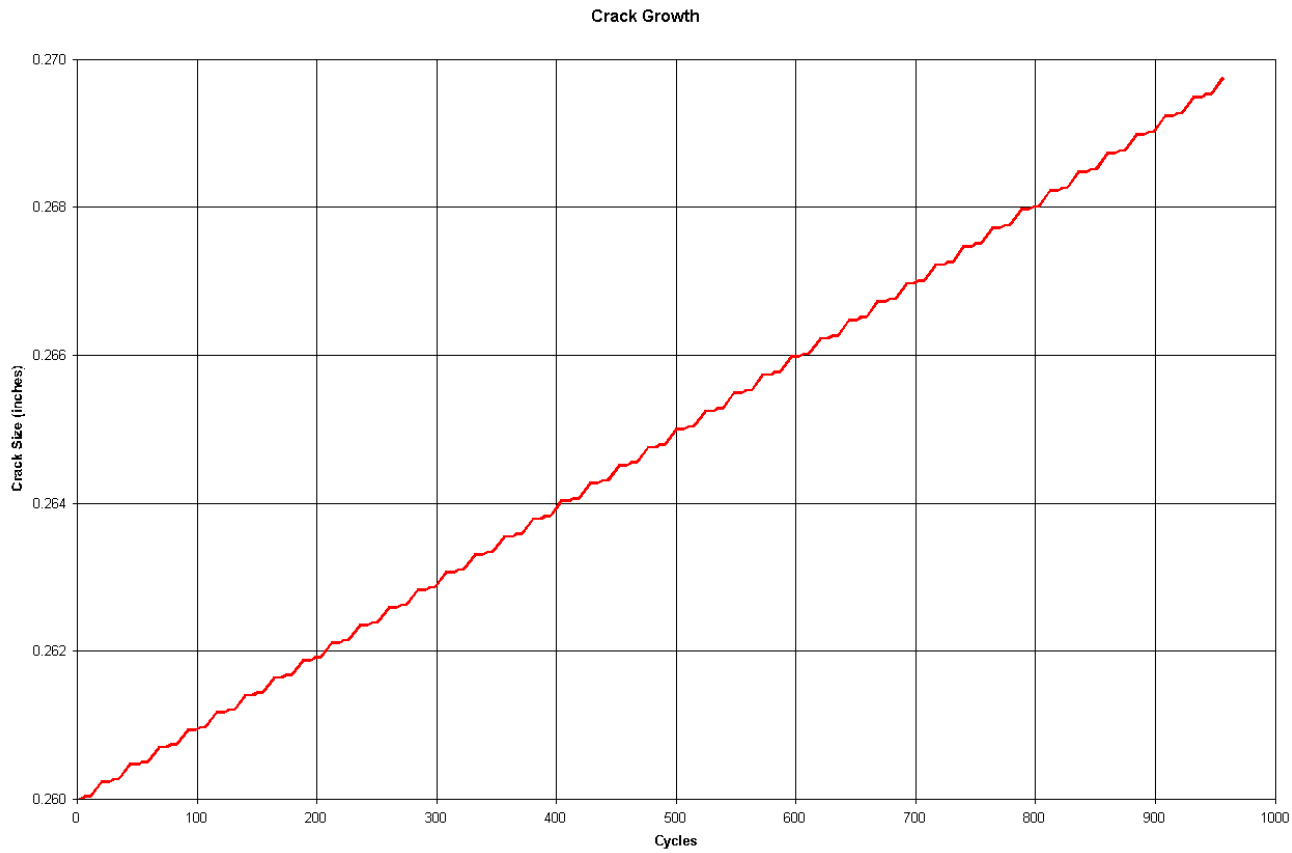

Figure 6-13: Fatigue Crack Growth Results (Axial Flaw)

7.0 SUMMARY AND CONCLUSIONS

The evaluations contained in this report form the basis for the weld overlay design for the HNP-2 DMW weld N2G. The evaluations were performed in accordance with the requirements of Generic Letter 88-01 (including Supplement 1), NUREG-0313, Revision 2 [5], BWRVIP-75 [17], and the ISI-ALT-08-02 [3]. The following are the conclusions of these evaluations.

- The weld overlay design meets all the design requirements of Generic Letter 88-01 and NUREG-0313 for "Standard" overlays. The overlay also meets all the design requirements of ISI-ALT-08-02 [3].

- The effect of the application of the weld overlay will increase the total mass at this location by an insignificant amount.

The above conclusions indicate that the weld overlay implementation at HNP-2 complies with the provisions and requirements of Generic Letter 88-01, NUREG-0313, Revision 2, BWRVIP-75, ASME, Section III, and ASME, Section XI.

8.0 REFERENCES

1. SI Calculation 0900556.301, Rev. 0, "Weld Overlay Design for Hatch Unit 2 Recirculation Inlet Nozzle N2G."

2. ASME Boiler and Pressure Vessel Code, Section XI, 2001 Edition with Addenda up to and including 2003.

3. Southern Nuclear Operating Company, ISI-ALT-08-02, Version 1.0, "Proposed Alternative in Accordance with 10CFR 50.55a(a)(3)(i), Application of Dissimilar Weld Full-Structural Weld Overlays," SI File 0900556.202.

4. NRC Generic Letter 88-01, "NRC Position on IGSCC in BWR in Austenitic Stainless Steel Piping," January 1988, with Supplement 1, February 4, 1992.

5. NRC Document No. NUREG-0313, "Technical Report on Material Selection and Processing Guidelines for BWR Coolant Pressure Boundary Piping," Revision 2, January 1988.

6. ASME Boiler and Pressure Vessel Code, Code Case N-740, Full Structural Dissimilar Metal Weld Overlay for Repair or Mitigation of Class 1, 2, and 3 Items, Section XI, Division 1.

7. SI Calculation 0900556.303, Rev. 0, "Residual Stress Analysis of Hatch Unit 2 Recirculation Inlet Nozzle N2G with Weld Overlay Repair."

8. ANSYS Mechanical and PrepPost, Release 11.0 (w/Service Pack 1), ANSYS Inc., August 2007.

9. GE/Hitachi Report No. H2R20-APR-014, Examination Summary Sheet, SI File No. 0900556.203.

10. Combustion Engineering, Inc. Report No. CENC-1232, "Analytical Report for Hatch No. 2 Reactor Vessel for Georgia Power Company," April 1975, SI File No. 0900556.201.

11. SI Calculation No. 0800777.307, Rev. 1, "Material Properties for Residual Stress Analyses, Including MISO Properties Up To Material Engineering Ultimate Tensile Strength".

12. SI Calculation Package 0900556.302, Rev. 0, "Thermal and Unit Mechanical Stress Analyses for Hatch Unit 2 Recirculation Inlet Nozzle N2G with Weld Overlay Repair."

13. ASME Boiler and Pressure Vessel Code, Section III, 2001 Edition with Addenda through 2003.

14. SI Calculation Package 0900556.304, Rev. 1, "Code Compliance and Crack Growth Evaluation of RPV Recirculation Inlet Nozzle N2G with Weld Overlay Repair."

15. ASME Boiler and Pressure Vessel Code, Section II, Part D, Material Properties, 2001 Edition with Addenda through 2003.

16. **pc-CRACK™** for Windows, Version 3.1-98348, Structural Integrity Associates, 1998.

17. BWR Vessel and Internals Project: Technical Basis for Revisions to Generic Letter 88-01 Inspection Schedule (BWRVIP-75)," EPRI, Palo Alto, CA and BWRVIP:1999 TR-113932, October 1999.

18. NUREG/CR-6721, 'Effects of Alloy Chemistry, Cold Work, and Water Chemistry on Corrosion Fatigue and Stress Corrosion Cracking of Nickel Alloys and Welds,' Argonne National Laboratory, Argonne, IL, April 2001.

19. BWRVIP-59-A: BWR Vessel and Internals Project, Evaluation of Crack growth in BWR Nickel Base Austenitic Alloys in RPV Internals, EPRI, Palo Alto, CA: 1998. TR-108710, SI File No. BWRVIP-01-259P.

20. GE Nuclear Document GE-NE-A13-00402-9B, "Extended Power Uprate Evaluation Task Report For Edwin I. Hatch Plant Unit 2, Reactor Pressure Vessel Stress Report Reconciliation," Revision 0, March 1998, SI File No. 0900556.204.

21. C. M. Brown and W. J. Mills, 'Fracture Toughness, Tensile and Stress Corrosion Cracking Properties of Alloy 600, Alloy 690 and Their Welds in Water,' Paper 90, Corrosion, The NACE International Annual Conference and Exposition, 1996.